



**TRIBHUVAN UNIVERSITY  
INSTITUTE OF ENGINEERING  
CENTRAL CAMPUS, PULCHOWK**

**THESIS NO.: 070MSCS666**

**Super Resolution Image Reconstruction**

**By  
Sunena Gwachha**

**A THESIS  
SUBMITTED TO THE DEPARTMENT OF ELECTRONICS AND  
COMPUTER ENGINEERING IN PARTIAL FULFILMENT OF THE  
REQUIREMENTS FOR THE DEGREE OF MASTER OF SCIENCE IN  
COMPUTER SYSTEM AND KNOWLEDGE ENGINEERING**

**DEPARTMENT OF ELECTRONICS AND COMPUTER ENGINEERING  
LALITPUR, NEPAL**

**NOVEMBER, 2015**

## ABSTRACT

Super Resolution is a process to increase the resolution of an image using information from several different images. Each low resolution images has new information of the image and the main aim of super resolution is to combine these low resolution images to enhance the image resolution.

In this thesis work, evaluation of different reconstruction based super resolution algorithms in order to enhance the low resolution images is done by experiments using simulated and real low resolution images. The observation model generates different simulated low resolution images obtained by rotation, translation, blurring and adding noise on high resolution image. For motion estimation different image registration algorithms (Vandewalle et al, Marcel et al and Keren et al) are applied to those simulated low resolution images. The parameters obtained from image registration are used to reconstruct the high resolution on different image reconstruction algorithm (Interpolation, Papoulis Gerchberg, Iterated Back Projection (IBP), Robust Super Resolution, Projection onto Convex Sets (POCS)). The obtained images are passed through Median filter and Weiner filter to remove blur and noise. The result is then compared and analyzed by means of objective image quality criteria mean square error(MSE) and peak signal to noise ratio(PSNR). The overall process is repeated for reconstruction of the real low resolution images. Finally, the obtained result is examined to show the performance of algorithms.

### **Keywords:**

Super Resolution, Motion Estimation, Image Registration, Image Reconstruction

## **ACKNOWLEDGEMENT**

First of all, I would like to express my deep gratitude to Department of Electronics and Computer Engineering for providing the opportunity to carry out thesis work as a partial fulfillment of Master of Science in Computer Systems and Knowledge Engineering.

I would like to express my sincere gratitude to the contribution of my thesis Supervisor and the Program Coordinator, Dr. Sanjeeb Prasad Panday. I am indebted to him for providing encouragement, outstanding supervision, expert guidance, consistent supports and constructive criticism since the beginning of the thesis.

I am also grateful to our head of department, Dr. Dibakar Raj Pant, Prof. Dr. Shashidhar Ram Joshi, Prof. Dr. Subarna Shakya, Dr. Arun K. Timilsina, Dr. Aman Shakya and Dr. Basanta Joshi for their encouragement and valuable guidance.

Likewise, I would like to extend my appreciation to all of my friends for their advice and encouragement in this thesis work.

Finally, a special thanks to my family for supporting me and encouraging me with their blessings to accomplish this work.

Sunena Gwachha  
(070/MSCS/666)

# TABLE OF CONTENTS

Abstract .....	i
Acknowledgement .....	ii
List of Tables .....	v
List of Figures .....	vi
List of Abbreviations .....	vii
CHAPTER 1 – INTRODUCTION .....	1
1.1 Background .....	1
1.2 Problem Statement .....	2
1.3 Objectives .....	2
1.4 Scope of the Work .....	2
1.5 Organization of Report .....	3
CHAPTER 2 – LITERATURE REVIEW .....	5
2.1 Related Work .....	5
CHAPTER 3 – METHODOLOGY .....	8
3.1 Working Principle .....	8
3.2 Image Acquisition Model .....	9
3.2.1 Blur Model .....	10
3.2.1.1 Average Blur .....	10
3.2.1.2 Gaussian Blur .....	10
3.2.1.3 Motion Blur .....	11
3.2.2 Noise Model .....	11
3.3 Image Registration .....	11
3.3.1 Vandewalle algorithm .....	12
3.3.2 Marcel algorithm .....	12
3.3.3 Keren algorithm .....	12
3.4 Super Resolution Methods .....	12
3.4.1 Interpolation .....	13
3.4.2 Papoulis Gerchberg .....	13
3.4.3 Iterated Back Projection(IBP) .....	14
3.4.4 Robust Super Resolution .....	15
3.4.5 Projection onto Convex Sets (POCS) .....	16
3.5 Deblurring and Denoising .....	16

3.5.1 Wiener Filter .....	17
3.5.2 Median Filter .....	17
3.6 Similarity Analysis Techniques .....	17
3.6.1 Mean Square Error (MSE) .....	18
3.6.2 Peak Signal to Noise Ratio (PSNR) .....	18
CHAPTER 4 – RESULTS AND DISCUSSIONS .....	20
4.1 Test Based on Simulated Images.....	20
4.1.1 Experiment Results .....	20
4.2 Test Based on Real Images .....	42
4.2.1 Experiment Results .....	42
4.3 Discussion .....	49
CHAPTER 5– CONCLUSION AND RECOMMENDATION .....	52
5.1 Conclusion .....	52
5.2 Limitation .....	53
5.2 Recommendation .....	53
REFERENCES .....	54
APPENDIX A .....	56
APPENDIX B .....	57
APPENDIX C .....	67

## LIST OF TABLES

<b>TABLES</b>		<b>PAGE</b>
Table 4.1	Comparison of methods based on quality metrics	21
Table 4.2	Comparison of different methods based on quality metrics for sample 2 Image	23
Table 4.3	PSNR values for table 4.2	24
Table 4.4	MSE and PSNR values for different noise level	26
Table 4.5	Comparison of results obtained by Median and Weiner filtering methods for figure 4.9	27
Table 4.6	PSNR values for the results obtained in Table 4.5	39
Table 4.7	Comparison of results obtained by Median and Weiner filtering methods for figure 4.11	30
Table 4.8	PSNR values for the results obtained in table 4.7	31
Table 4.9	Comparison of results obtained by Median and Weiner filtering methods for figure 4.13	33
Table 4.10	PSNR values for the results obtained in table 4.9	34
Table 4.11	PSNR values for the results obtained by Median and Weiner filtering methods	36
Table 4.12	Comparison of different methods based on quality metrics for figure 4.22	42
Table 4.13	Comparison of different methods based on quality metrics for figure 4.23	44
Table 4.14	Comparison of different methods based on quality metrics for figure 4.24	46
Table 4.15	Comparison of different methods based on quality metrics for figure 4.25	47

## LIST OF FIGURES

<b>FIGURES</b>	<b>PAGE</b>
Figure 1.1 Basic scheme of super resolution	1
Figure 3.1 Sub pixels shift	8
Figure 3.2 The observation model relating low resolution images to high resolution counter parts [2]	9
Figure 3.3 Block diagram of Papoulis Gerchberg Algorithm	14
Figure 4.1 (a) Sample 1 HR image (b) (c) (d) (e) LR images with random transformation	20
Figure 4.2 Reconstructed HR images (a) Interpolation (b) Papoulis Gerchberg (c) Iterated Back Projection (d) Robust SR (e) POCS	21
Figure 4.3 Bar graph of table 4.1	22
Figure 4.4 (a) Sample 2 HR image (b) (c) (d) (e) LR images with random Transformation	22
Figure 4.5 Plot of table 4.3	24
Figure 4.6 (a) Sample HR image (b) 10 db (c) 20 db (d) 30 db (e) 40 db LR images with random transformation	25
Figure 4.7 Reconstructed Images using POCS algorithm (a) 10 db (b) 20 db (c) 30 db (d) 40 db noise	25
Figure 4.8 Bar graph of noisy image using Keren motion estimation reconstructed through POCS	26
Figure 4.9 Original and transformed images (a) HR image and down sampled with transformation (b) 10, (2.13, 3.92) pix (c) 20, (4.67, 6.71) pix (d) 50, (9.87, 1.39) pix LR images (e) 100, (6.59, 8.83) pix LR images	27
Figure 4.10 Bar graph of table 4.6	29
Figure 4.11 (a) Sample 4 HR image (b) (c) (d) (e) LR images with random transformation with motion blur and 10 db noise	30
Figure 4.12 Bar graph of table 4.8	32
Figure 4.13 (a) Sample 5 HR image (b) (c) (d) (e) LR images with random transformation with average blur and 20 db noise	32
Figure 4.14 Bar graph of table 4.10	34

Figure 4.15	(a) Sample 5 HR image (b) (c) (d) (e) LR images with random transformation with average blur and 20 db noise	35
Figure 4.16	Reconstructed Images (a) Interpolation (b Papoulis Gerchberg (c) Iterated Back Projection (d) Robust Super Resolution (e) POCS	35
Figure 4.17	Effect of image quality for Interpolation method	37
Figure 4.18	Effect of image quality for Papoulis Gerchberg method	38
Figure 4.19	Effect of image quality for IBP method	39
Figure 4.20	Effect of image quality for Robust SR method	40
Figure 4.21	Effect of image quality for POCS method	41
Figure 4.22	Sample 1 Real LR images	41
Figure 4.23	Sample 2 Real LR images	44
Figure 4.24	Sample 3 Real LR images	45
Figure 4.25	Sample 4 Real LR images	47



## LIST OF ABBREVIATIONS

HR	High Resolution
IBP	Iterated Back Projection
Keren	Image Registration Method developed by Keren et al
LR	Low Resolution
Marcel	Image Registration Method developed by Marcel et al
MSE	Mean Square Error
POCS	Projection onto Convex Sets
PSNR	Peak Signal to Noise Ratio
SR	Super Resolution
Vandewalle	Image Registration Method developed by Vandewalle et al

**CHAPTER 1**  
**INTRODUCTION**

# 1. Introduction

## 1.1 Background

Super resolution refers to produce high quality images from a set of low quality images. Naturally there is always a demand for better quality images. However, the hardware for high resolution images is expensive and can be hard to obtain. The resolution of digital photographs is limited by the optics of the imaging device. In conventional cameras, the resolution depends on CCD sensor density, which may not be sufficiently high. As the image capturing environment is not ideal, many distortions are also present in the low-resolution images [1]. They may have blurred, noisy, aliased low resolution captures of the scene. Therefore, a new approach is required to increase the resolution of the image. It is possible to obtain an high resolution image from multiple low resolution images by using the signal processing technique called super resolution. Generally all super resolution has the following basis steps as in figure 1.1 based upon the scheme of research and include are exclude some of these steps [2].

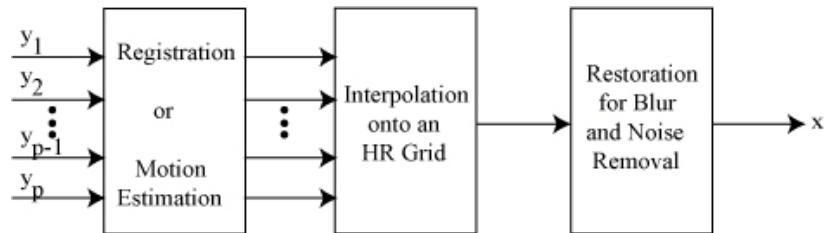


Figure 1.1: Basic scheme of super resolution

Motion estimation is essential to enable motion compensated filtering. It determines the relative shift between low resolution images and registers the pixels from all available low resolution images into common reference grid. The pixels of the low resolution images are usually non-uniformly distributed with respect to the reference grid. So the motion compensation and wrapping of the input low resolution images into reference grid is necessary. Restoration of the low resolution images is necessary to reduce the artifacts due to blurring and sensor noise. The filtering is done to improve image quality. Interpolation of the low resolution images with a predetermined zoom factor is applied to obtain the desired high resolution image. The fusion of the pixel values from the low resolution images is essential. This operation is at the heart of all super resolution algorithms.

## **1.2 Problem Statement**

Super resolution technology origins from the field of image restoration. The increasing difficulties in the resolution improvement by hardware prompts the super resolution reconstruction that can solve this problem effectively, but the general algorithms of super resolution reconstruction model are unable to quickly complete the image processing. Based on this problem, different super resolution reconstruction algorithm is studied in this thesis work. This study examines the super resolution algorithm as the cascade of two steps image registration and image reconstruction.

## **1.3 Objectives**

The prime objectives of this thesis are:

- i. To implement and compare some of the well known super resolution techniques in standard and real images.
- ii. To study the different blur and noise on the low resolution images and to recover them.

## **1.4 Scope of the Work**

The scope of the thesis is on the implementation and comparison of different super resolution techniques. This study examines the SR schemes as the cascade of two steps image registration and image reconstruction. The two steps will be covered in detail. The main objective is to understand and distinguish the advantages and disadvantages of major super resolution methods.

A MATLAB GUI has been implemented to test the super resolution techniques. With the help of the implementation, methods have been critically examined and some additions have been made to improve the visual quality. Besides the comparison and analysis of the super resolution methods, the robustness of the methods under different blurring and noisy conditions has also been examined and resolved using different filter in this thesis.

## **1.5 Organization of Report**

The chapter 1 of this thesis report is Introduction that describes a brief introduction to super resolution and the objectives. The definition of the problem has been included in this chapter. Chapter 2 basically includes the relevant literature studied and referred in the course of this research work.

Chapter 3 is the methodology section that discuss the image acquisition process of low resolution images. The types of blur, noise and some image registration methods and reconstruction methods are examined. It includes the similarity analysis techniques used in this thesis work.

Chapter 4 includes the Results and Discussion of the different approaches of super resolution and their analysis and comparison are given. The methods are compared using artificially generated images and some real low resolution images. And finally, Chapter 5 includes the conclusion of the thesis and recommendations for future researches in the area.

**CHAPTER 2**  
**LITERATURE REVIEW**

## 2. Literature Review

### 2.1 Related Work

The term super resolution generally refers to the problem of receiving image spectrum beyond the diffraction limit through the use of signal processing techniques. In this thesis the focus is on super resolution reconstruction, which consist the process of creating a high resolution image from a sequence of low resolution images. So, the related works based on super resolution image reconstruction are described below.

Tsai and Huang were the first to consider the problem of obtaining a high quality image from several lower quality and translationally displaced images [3]. Their data set consisted of terrestrial photographs taken by Landsat satellites. They modeled the photographs as aliased, translationally displaced versions of a constant scene. Their approach consisted in formulating a set of equations in the frequency domain, by using the shift property of the Fourier transform. Optical blur or noise was not considered.

Changh, Y. Ngdy, Xiongym [4] introduced the idea of Neighbor Embedding in manifold learning in super resolution reconstruction assuming that LR and HR image block have similar manifold structure, getting the training set of LR image and HR image block through the image training then searching the k neighbor blocks in training set of LR image block to be reconstructed and solving their neighbor coefficients and with linear combination of coefficients and k corresponding HR neighbor block of HR training set to obtain HR block after matching reconstruction. The advantages of this method that the number of training set is small and reconstruction time is relatively short but the reconstruction exists the over fitting and under fitting phenomenon.

Later the compressed sensing [5] was introduced into the super-resolution reconstruction, and Yang et al [6] used the linear programming and low resolution dictionary to solve the sparse representation of low resolution image block to be reconstructed, using sparse representation coefficients and the corresponding high resolution image block to finishing image reconstruction. This algorithm was advantageous in its no need to set the block number of a low resolution image for the sparse representation, but the construction of the dictionary is random and unpopular.

Rhee and Kang[7] adopted Discrete Cosine Transform in order to decrease the operand and increase the efficiency of algorithm. They overcome the lack of frames by low resolution sampling and ill condition reconstruction of unknown sub pixel motion information by regularization parameter. The frequency domain method were with comparatively easy theories and low computational complexity. The disadvantage of these methods is that it can only handle some condition of global motion. The loss of data dependency in the frequency domain made the application of prior information in regularization ill conditioned problem difficult.

Lucchese and Cortelazzo[8] develop a rotation estimation algorithm based on the property that the magnitude of Fourier transform of image and the mirror version of magnitude of Fourier transform of a rotated image have a pair of orthogonal zero crossing lines. The angle that these links makes with the axes is equal to the half of the rotation angle between the two image. The horizontal and vertical shifts are estimated afterwards using a standard phase correlation methods.

Spatial domain methods enjoy better handling of noise, and a more natural treatment of the image point spread blur in cases where it cannot be approximated by a single convolution operation on the high resolution image. They use a model of how each offset low resolution pixel is derived from the high resolution image in order to solve for the high resolution pixel values directly. They use a model of how each offset low resolution pixel is derived from the high resolution image in order to solve for the high resolution pixel values directly. Here in this thesis work, different spatial domain based super resolution algorithm are studied and evaluated by experimenting with different low resolution images.



**CHAPTER 3**  
**METHODOLOGY**

### 3. Methodology

#### 3.1 Working Principle

The basic premise for increasing the resolution in SR techniques is the availability of multiple low resolution images captured from the same scene. In SR, typically, the low resolution images represent different “looks” at the same scene. That is, low resolution images are sub-sampled (aliased) as well as shifted with sub-pixel precision as shown in figure 3.1[2]. If the low resolution images are shifted by integer units, then each image contains the same information, and thus there is no new information that can be used to reconstruct a high resolution image. If the low resolution images have different sub pixel shifts from each other and if aliasing is present, however, then each image cannot be obtained from the others. In this case, the new information contained in each low resolution image can be exploited to obtain an high resolution image. To obtain different looks at the same scene, some artificial images are generated by sub-pixel shifts. In addition, video camera can be used to capture a series of pictures, giving sufficiently rich sets of sub-pixel shifts between images. The camera will not be static during the image acquisition or at least the shots of the scene will be taken from different locations [2].

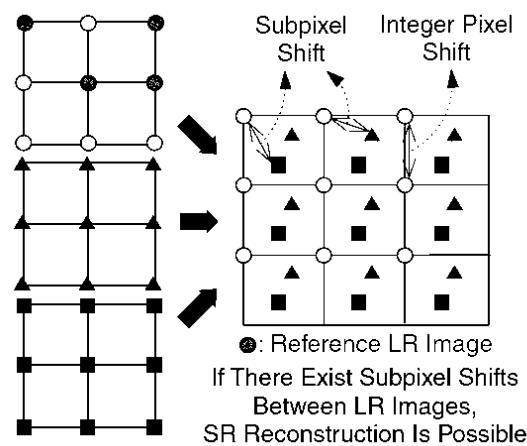


Figure 3.1: Sub pixels shift

### 3.2 Image Acquisition Model

The captured images are inverted at the first step. This inverting process requires a modeling of the relation between the high and the low-resolution images. The acquisition of an image has many details to consider. For example, optical distortions through the optics of the camera, aliasing effect inside the sensor, blurring caused by the unwanted camera shaking and scene motion, additional noise through every part of the pipeline plus the under-sampling of the camera make the captured images suffer from spatial resolution loss.

Assuming  $y_k$ , where  $k=1\dots p$  as the  $p$  low-resolution images and  $x$  as the real world high resolution observation that it is try to reach as close as possible at the end of the process. During the observation of the scene, assuming that  $x$  remains constant. By this way, all of the  $p$  observations are of the same scene. All of the differences between low resolution images are due to varying imaging conditions of the camera. In addition, the unknown noise is always present on all of the low resolution images. As a result, it will have  $p$  different observations of  $x$ . This model of observation can be represented in equation (3.1)[2] as:

$$y_k = DB_k M_k x + n_k \text{ for } k=1,2,\dots,p \dots\dots\dots (3.1)$$

Where  $M_k$  is a transformation matrix, which transforms  $x$  in vertical and horizontal shifts and scale variances as well as rotational motions in all 3D coordinate axes.  $B_k$  is the blur matrix that can be a result of optical disorder, fast motion, point spread function (PSF) of the sensor etc.  $D$  is the sub-sampling matrix that is the cause of the loss in spatial resolution. In addition,  $n_k$  represents the noise, which is present at all times.

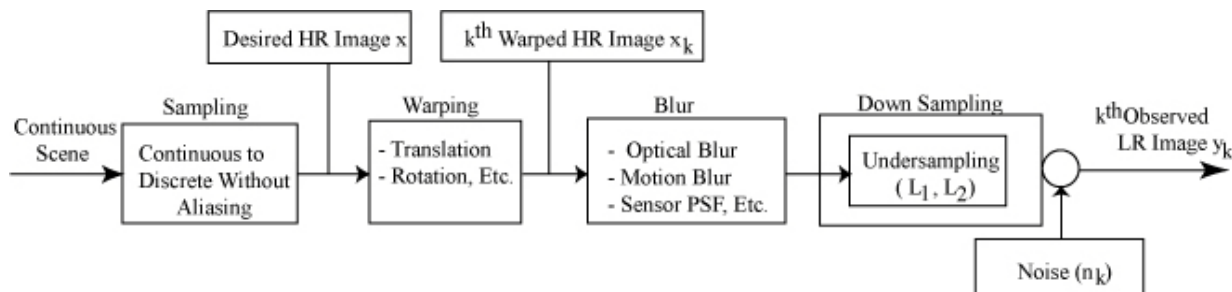


Figure 3.2: The observation model relating low resolution images to high resolution counter parts [2]

Alternatively, the observation model can be simplified to sum up all the effects in a single operator to make it easier to visualize the concept. This is possible if these models are unified in a simple matrix vector form since the low resolution pixels are defined as a weighted sum of the related high resolution pixels with additive noise. As a result, equation (3.1)[2] can be expressed as follows.

$$y_k = W_k x + n_k \text{ for } k=1,2,\dots,p \dots\dots\dots (3.2)$$

Where  $W_k$  is the effects of the blurring, sub-sampling and transformations takes place on the original high-resolution pixels of  $x$ . Again,  $n_k$  is the additive noise coming from the environment.

### 3.2.1 Blur Model

Blur is un-sharp image area caused by camera or subject movement, inaccurate focusing, or the use of an aperture that gives shallow depth of field. The blur effects are filters that smooth transitions and decrease contrast by averaging the pixels next to hard edges of defined lines and areas where there are significant color transition.

The types of blurs considered in this thesis are classified as follows:

- i. Average Blur
- ii. Gaussian Blur
- iii. Motion Blur

#### 3.2.1.1 Average Blur

The Average blur is use to remove noise and specks in an image. This type of blurring can be distribution in horizontal and vertical direction and can be circular averaging by radius  $R$  which evaluated by the formula [9]:

$$R = \sqrt{h^2 + v^2} \dots\dots\dots (3.3)$$

where  $h$  is the horizontal size blurring direction and  $v$  is vertical blurring size direction is the radius size of the circular average blurring.

#### 3.2.1.2. Gaussian Blur

The Gaussian blur is a type of image blurring filter that uses a Gaussian function for calculating the transformation to apply to each pixel in the image. Gaussian blur is that pixel weights aren't equal they decrease from kernel center to edges according to a bell-shaped curve. The Gaussian blur effect is a filter that blends a specific number of pixels

incrementally, following a bell-shaped curve. The blurring is dense in the center and feathers at the edge. Gaussian blur depends on the size and alfa [9].

### 3.2.1.3 Motion Blur

It occurs when there is relative motion between the object and the camera during exposure. The many type of motion blur can be distinguished all of which are due to relative motion between the recording device and the scene. This can be in the form of translation, a rotation, a sudden change of scale, or some combinations of these. The Motion blur effect is a filter that makes the image appear to be moving by adding blur in a specific direction [9].

### 3.2.2 Noise Model

Image noise is random variation of brightness or color information in images, and is usually an aspect of electronic noise. It can be produced by the sensor and photon detector. Image noise is an undesirable by product of image capture that adds spurious and extraneous information. The standard model of amplifier noise is additive, white Gaussian, independent at each pixel and independent of the signal intensity. This type of noise has a Gaussian distribution, which has a bell shaped probability distribution function given by equation (3.4).

$$F(g) = \frac{1}{\sqrt{2\pi}\sigma} e^{-\frac{(g-m)^2}{2\sigma^2}} \dots\dots\dots (3.4)$$

where g represents the gray level, m is the mean or average of the function, and σ is the standard deviation of the noise.

## 3.3 Image Registration

Image registration is the method of aligning multiple images on the same grid. Registering frames of a images from a sequence is mainly about solving the problem of geometric relation with the reference image and finding the right way to put them on the same geometrical grid.

Image Registration Algorithms considered in this thesis are classified as follows:

- i. Vandewalle Algorithm
- ii. Marcel Algorithm
- iii. Keren Algorithm

Then the image registration algorithms are compared with artificially generated images. During the generation of these synthetic images, different transformation parameters like rotation, translation and scaling is implemented.

### **3.3.1 Vandewalle algorithm**

Vandewalle algorithm uses the property that a shift in the space domain is translated into a linear shift in the phase of the image's Fourier Transform. Similarly, a rotation in the space domain is visible in the amplitude of the Fourier Transform. Hence, the Vandewalle algorithm computes the image's Fourier Transforms and determines the 1-D shifts in both their amplitudes and phases [10].

### **3.3.2 Marcel algorithm**

Most of the frequency domain registration methods are based on the fact that two shifted images differ in frequency domain by a phase shift only, which can be found from their correlation. Using a log-polar transform of the magnitude of the frequency spectra, image rotation and scale can be converted into horizontal and vertical shifts. These can therefore also be estimated using a phase correlation method [11].

### **3.3.3 Keren algorithm**

The Keren algorithm uses different down sampled versions of the images to be analyzed in order to achieve its goal. First a 4x down sampled version of the images is used to perform an estimation of the shift and rotation using Taylor series. The same is done with 2x down sampling, but after correcting for the shifts and rotations estimated earlier. Finally, the same is done with the full resolution images, in order to further fine-tune the estimates [12].

## **3.4 Super resolution methods**

The resolution improvement is the process of magnifying the image into a larger size. In the process of resolution enhancement, a number of pixels is available. Then an empty grid of the targeted high resolution image depending on these pixels is created. According to the available low resolution pixel intensities, the entire image is filled pixel by pixel. At the end, a higher resolution image is achieved, which has pixel values based on the available pixels. There are different pixel filling methods. Depending on how the empty grid is filled, the resolution enhancement methods used in this is classified as follows.

- i. Interpolation
- ii. Papoulis Gerchberg
- iii. Iterated Back Projection (IBP)
- iv. Robust Super Resolution
- v. Projection onto Convex Sets (POCS)

### 3.4.1 Interpolation

This methods aligns all the images pixels on a high resolution grid and then applies a bicubic interpolation. It uses a 4 by 4 neighborhood to find the missing pixels in the high resolution grid. It uses a polynomial passing through four pixels to make a decision. Therefore, it creates enlarged images that are smoother and higher quality. The following equation (3.5)[10] is the continuous time convolution kernel of the cubic interpolation. When the interpolation is separately applied to rows and columns of an image, the bicubic interpolation is obtained [13].

$$h(t) = \begin{cases} \frac{3}{2} |t|^3 - \frac{5}{2} |t|^2 + 1 & 0 \leq |t| \leq 1 \\ -\frac{1}{2} |t|^3 + \frac{5}{2} |t|^2 - |t| + 2 & 1 \leq |t| \leq 2 \\ 0 & |t| > 2 \end{cases} \dots\dots\dots (3.5)$$

### 3.4.2 Papoulis Gerchberg

This method cuts the high frequencies by situating the given pixels on a high resolution grid goes into the frequency domain, and it is assumed that the missing data correspond to a missing region in the frequency domain [14].

This method, assumes two things:

- 1 Some of the pixel values in the high-resolution grid are known.
- 2 The high frequency components in the high-resolution image are zero.

It works by projecting HR grid data on the two sets described above. The steps are:

Step 1: Form a high resolution grid. Set the known pixels values from the low resolution images (after converting their pixel position to the reference frame of first low resolution image). The position on the HR grid is calculated by rounding the magnified pixel positions to nearest integer locations [14].

Step 2: Set the high-frequency components to zero in the frequency domain.

Step 3: Force the known pixel values in spatial domain.

Repeat from steps 1.

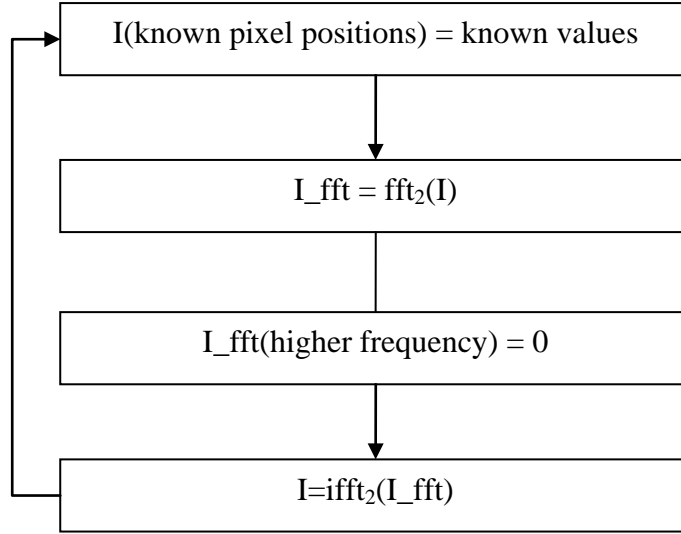


Figure 3.3: Block diagram of Papoulis Gerchberg Algorithm

### 3.4.3 Iterated Back Projection (IBP)

The idea behind iterated back projection reconstruction technique is estimation of high resolution image and then iteratively add it to the sum of errors between each low resolution image and the estimated high resolution image that went through suitable transforms that is given by motion estimations. First HR image is estimated and then LR images are synthetically formed from this HR image according to the observation model. The HR image is iteratively refined by back projecting the error i.e. the difference between synthetically formed LR images and observed LR images until the energy of the error is minimized. The back projection function is defined as [2]:

$$x^{n+1}[n_1, n_2] = x^n[n_1, n_2] + \sum_{k=1}^N (y_k[m_1, m_2] - y_k^n[m_1, m_2]) \times h^{BP} \dots\dots\dots (3.6)$$

where n is the iteration number, x is the simulated HR image, N is the number of images,  $y_k$  is the observed LR images and  $y_k^n$  is the final simulation of LR images after n iterations and  $n_1, n_2$  are the HR space and  $m_1, m_2$  is the LR space. Finally,  $h^{BP}$  is the back projection kernel where the LR image is mapped into HR grid, which is the mean and upsampled operation, used in study. However,  $h^{BP}$  may be utilized as an additional constraint, which represents the desired property of the solution [2].



The steps of Iterated Back Projection algorithm are:

- Step 1: Unregistered LR images are converted to registered LR images by applying homography matrices.
- Step 2: Get mean and upsample of the registered image as a simulated HR image.
- Step 3: Downsample the simulated image and apply inverse homographies to get simulated LR images.
- Step 4: Get the difference of simulated and observed LR images.
- Step 5: Apply homographies and register the residues.
- Step 6: Get mean and upsample the registered residues and apply back projection.
- Step 7: Add the upsampled gross residue to the simulated HR image.

#### **3.4.4 Robust Super Resolution**

Robust Super Resolution algorithm enhances the performance of IBP by incorporating a robust median estimator. Due to this additional step, the resolution can be improved resulting into more accurate estimates of HR images especially in the presence of outliers. The outliers may be due to inaccurate blur models or moving objects or noise. Since aliasing occurs in the regions having higher frequencies, so by treating each pixel in the estimated solution independently, it is ensured to improve the enhancement in the regions of high frequencies as aliasing is the main source of information for resolution enhancement. The pixel-wise median therefore performs better [15].

The steps of Robust SR algorithm are:

- Step 1: Choose one LR image as the reference image.
- Step 2: For every additional LR image, estimate the motion between the additional LR image and the reference LR image. Register additional LR image to the reference LR image using image registration algorithm, create the new HR image through bicubic interpolation between the registered LR image and the reference LR image.
- Step 3: Compute the median of the HR image as the updated super resolved image.
- Step 4: Enhance the super resolved image if necessary by sharpening edges and increasing contrast.

### 3.4.5 Projection onto Convex Sets (POCS)

The Projection onto Convex Sets (POCS) is another iterative method which employs prior knowledge of the solution. Each LR image defines a constraining convex set of possible HR images. When the convex sets are defined for all LR images, an iterative algorithm is employed to an intersection of the convex sets. It is assumed that HR image belongs to this intersection. The POCS technique uses the following algorithm to find a point within the intersection set given by an initial guess [2].

$$x^{k+1} = P_M P_{M-1} \dots P_2 P_1 x_k \dots \dots \dots (3.7)$$

where  $x_0$  is an initial guess,  $P_j$  is the projection of a given point onto the  $j$ -th convex set and  $M$  is the number of convex sets.

The steps of POCS algorithm are:

- Step 1: Unregistered LR images are converted to registered LR images by applying homographies.
- Step 2: Upsample the reference LR image as the simulated HR image.
- Step 3: For all LR images, apply the homographies to find the motion compensated pixel coordinates.
- Step 4: To the found motion compensated coordinates apply the Gaussian PSF for each pixel.
- Step 5: For every pixel in the image, find the difference between the simulated HR image pixels and Gaussian PSF applied pixels.
- Step 6: If difference  $> \delta$ , subtract  $\delta$  weight from that pixel.  
           If difference  $< \delta$ , add  $\delta$  weight to that pixel.  
           If difference =  $\delta$ , leave as it is.
- Step 7: Normalize the HR pixel value to the intensity space [0 255].
- Step 8: Update the simulated HR image and repeat from step 4.

### 3.5 Deblurring and Denoising

A blurred or degraded image can be approximately described by this equation (3.8):

$$g(x,y) = \text{PSF} * f(x,y) + \rho(x,y) \dots \dots \dots (3.8)$$

where  $g$  is the blurred image, PSF distortion operator is called Point Spread Function,  $f$  is the original true image and  $\rho$  is additive noise, introduced during image acquisition, that

corrupts the image. Point Spread Function (PSF) is the degree to which an optical system blurs (spreads) a point of light.

The deblurring and denoising method used in thesis are as follows:

- i. Wiener Filter
- ii. Median Filter

### 3.5.1 Wiener Filter

Wiener filter is the technique for removal of blur in images due to linear motion or unfocused optics. It is also a standard image restoration technique for reconstructing the degraded image in the presence of known PSF. It removes or reduces to some extent the additive noise and inverts the blurring simultaneously. Wiener filter not only performs the deconvolution by inverse filtering (high pass filtering) but also removes the noise with a compression operation (low pass filtering). It compares with an estimation of the noiseless image we want or desired. The input to a wiener filter is a degraded image corrupted by additive noise [9] .

The wiener filter is defined by the following expression(3.9):

$$F(u, v) = \left[ \frac{H(u,v)^*}{|H(u,v)|^2 + [s_n(u,v)/s_f(u,v)]} \right] G(u, v) \dots\dots\dots (3.9)$$

$G(u,v)$  and  $H(u,v)$  are degraded image and degradation function respectively.  $S_n$  and  $S_f$  are the power spectra of noise and original image (before adding of noise). The wiener filter assumes the noise and power spectra of the object a prior.

### 3.5.2 Median Filter

The Median Filter is performed by taking the magnitude of all of the vectors within a mask and sorted according to the magnitudes. The pixel with the median magnitude is then used to replace the pixel studied. The median filter is given by (3.10) [16]:

$$\text{Median filter}(x_1 \dots x_N) = \text{Median}(\|x_1\|^2 \dots \|x_N\|^2) \dots\dots\dots (3.10)$$

## 3.6 Similarity Analysis Techniques

Similarity analysis is one of the important portions of this thesis. The reconstructed high resolution images from different algorithms are compared with the original high

resolution image using the different quality metrics. The error value given by the quality metrics are finally analyze and evaluate to know the degree of quality of reconstruction among the algorithm implemented.

Following approaches have been implemented in this thesis for image comparison.

### 3.6.1 Mean Square Error (MSE)

The mean square error (MSE) of an estimator measure the average of the square of the errors, that is difference between estimator and what is estimated.

In this thesis, MSE is used to compare original image and reconstructed image. MSE is calculated using following formula given by equation 3.11.

$$MSE = \frac{\sum_{x=1}^m \sum_{y=1}^N [I_m(x,y) - I'_m(x,y)]^2}{M.N} \dots\dots\dots (3.11)$$

where M, N stands for the size of the image in both horizontal and vertical axes,  $I_m$  is the original high resolution image and  $I'_m$  is the reconstructed high resolution image obtained by various algorithm that is to be examined.

### 3.6.2 Peak Signal to Noise Ratio (PSNR)

PSNR is defined as the ratio between the maximum possible power of signal and the power of corrupting noise that affects the fidelity of representation. Because many signal have wide dynamic range PSNR is usually expressed in term of logarithmic decibel scale.

PSNR is commonly used to measured the quality of reconstruction of images. The signal in this case is the original image data and the noise is the error introduced during the image acquisition process. Higher value of PSNR shows the better quality of reconstruction of image.

PSNR is calculated using following formula given by equation 3.12.

$$PSNR = 20 * \log_{10} \left[ \frac{255}{\sqrt{MSE}} \right] \dots\dots\dots (3.12)$$

**CHAPTER 4**  
**RESULTS AND DISCUSSIONS**

## 4. Results and Discussions

The experiments is done in the two steps. At first, the low resolution images are simulated from high resolution image using observation model. The obtained low resolution images are reconstructed using the algorithm mentioned in section 3.4. Then the same process is repeated on the real low resolution images. The obtained results from different algorithm are then compared and analyzed. The detail of all these procedures is described in detail below.

### 4.1 Test Based on Simulated Images

In this study, the synthetic LR images with known transformation parameters are used. As the motion parameters are fixed throughout the image, it is expected the image registration methods estimate these parameters as close as possible to the real values. Different 22 standard high resolution images are used to generate synthetic LR images during this study. The detail information about these HR images can be obtained from the link [WWW.flickr.com/photos/horiavarlan/sets](http://WWW.flickr.com/photos/horiavarlan/sets).

#### 4.1.1 Experiment Results

Several experiments are carried out to compare and analyze the performance of different super resolution reconstruction algorithm. For each experiments performance parameters are measured and plotted to compare with other methods.

Example 1

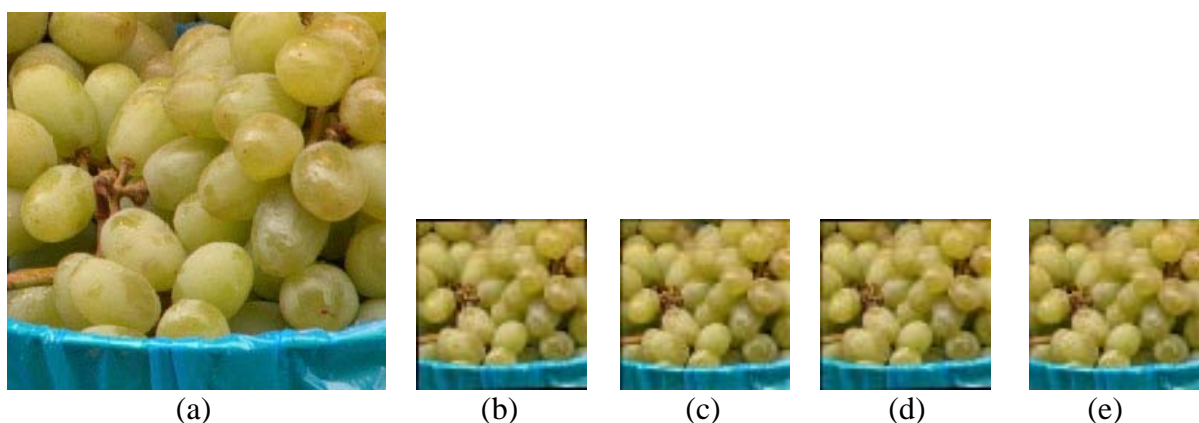


Figure 4.1: (a) Sample 1 HR image (b) (c) (d) (e) LR images with random transformation

In above figure, figure (a) is the sample HR image of dimension  $256 \times 256$ . Figures (b), (c), (d) and (e) are the LR images with random rotation and translation applied. Dimension of each LR image is reduced by factor 4.

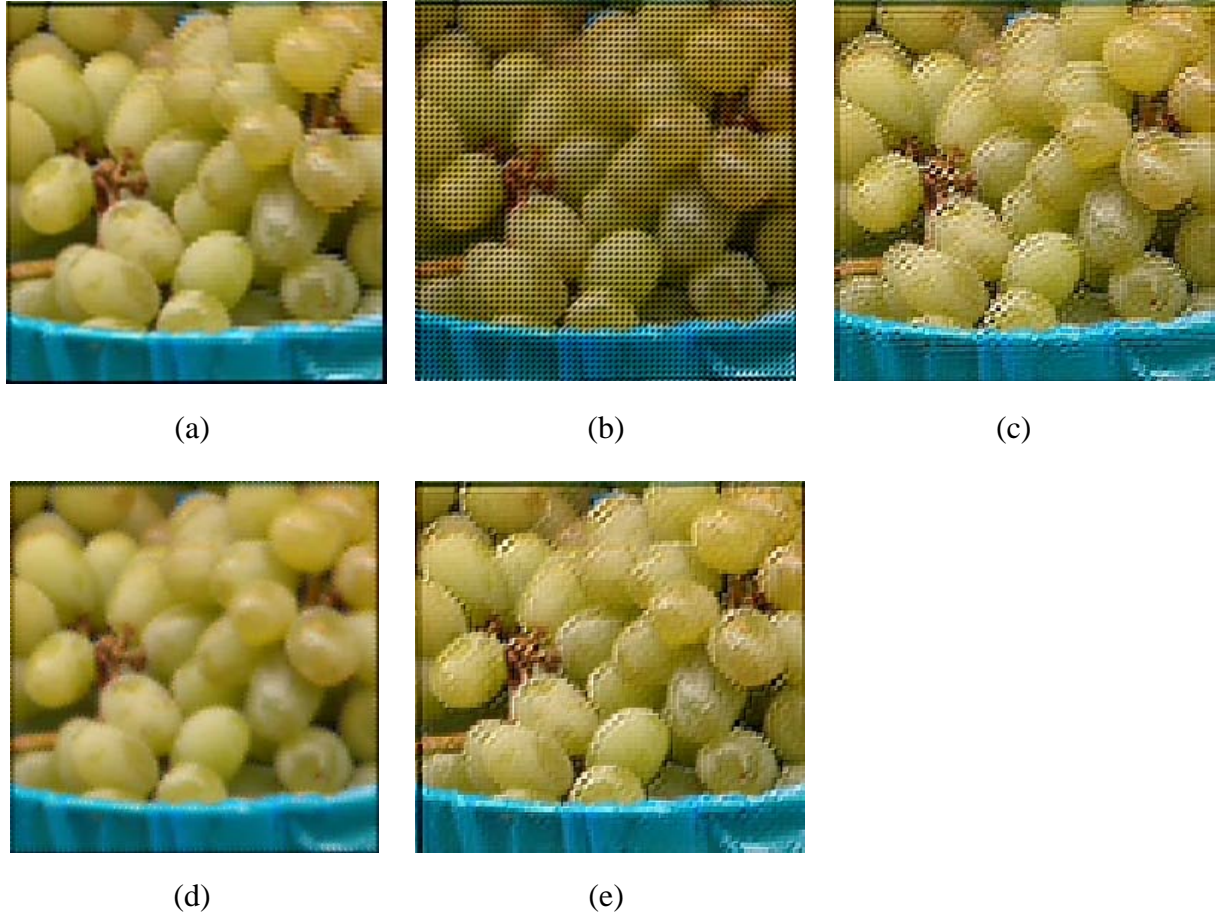


Figure 4.2: Reconstructed HR images (a) Interpolation (b) Papoulis Gerchberg (c) Iterated Back Projection (d) Robust SR (e) POCS

Vandewalle motion estimation algorithm is used to estimate the transformation parameters. These parameters are used in different image reconstruction algorithms to obtain HR image. Figure 4.2 shows different HR images reconstructed through different algorithms.

Table 4.1: Comparison of methods based on quality metrics

<b>Error/Reconstruction Algorithm</b>	<b>Interpolation</b>	<b>Papoulis Gerchberg</b>	<b>Iterated Back Projection</b>	<b>Robust Super Resolution</b>	<b>POCS</b>
MSE	41.81	168.94	70.66	56.81	42
PSNR	31.95	25.89	29.67	30.62	31.93

Above table shows the Mean Square Error (MSE) and Peak Signal to Noise Ratio (PSNR) obtained after using different algorithms for the sample image 1 with random transformation parameters and motion estimated through Vandewalle algorithm.

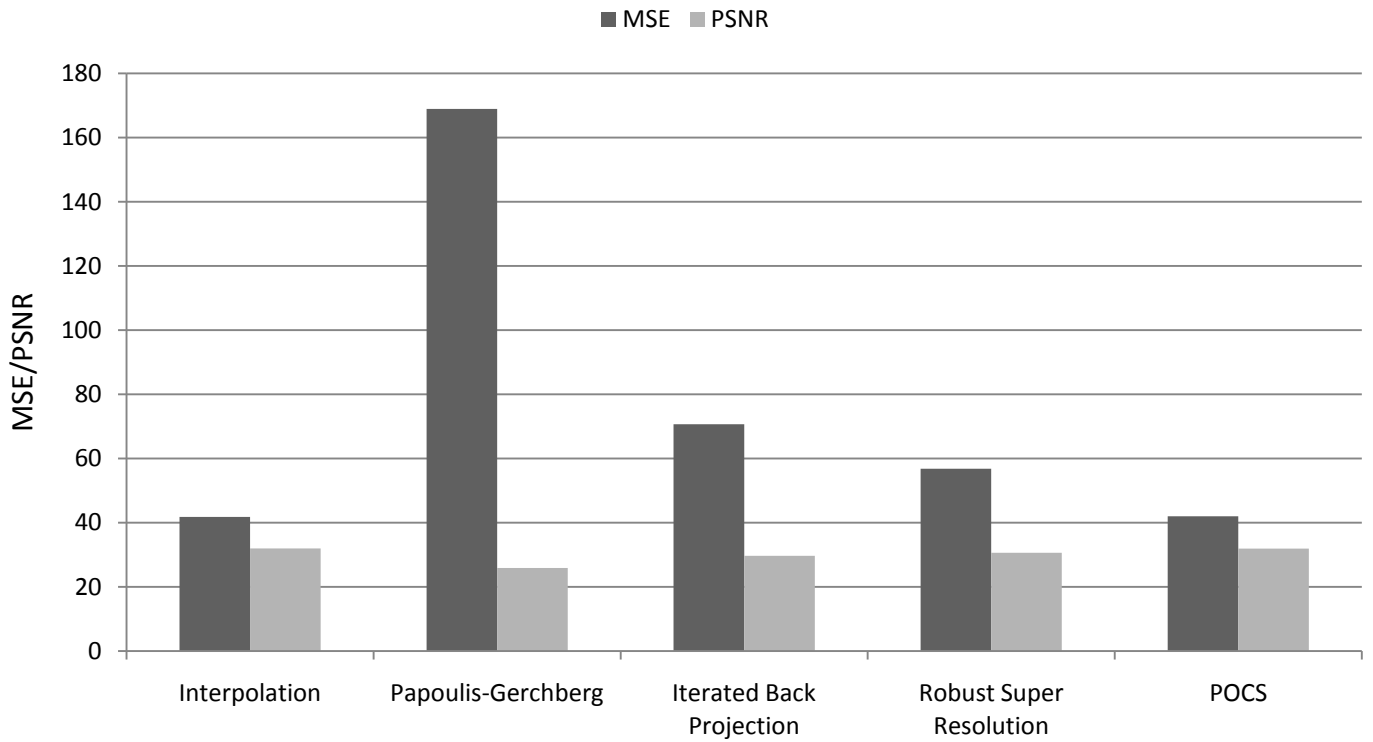


Figure 4.3: Bar graph of table 4.1

Figure 4.3 represents the table 4.1 in bar graph. From the bar graph it is observed that Interpolation and POCS algorithm has the least error compared to others.

#### Example 2

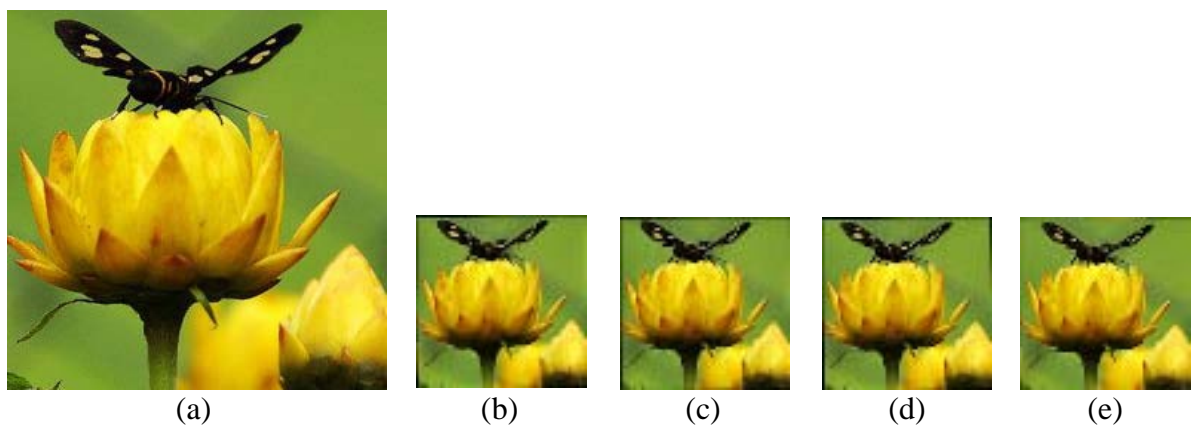

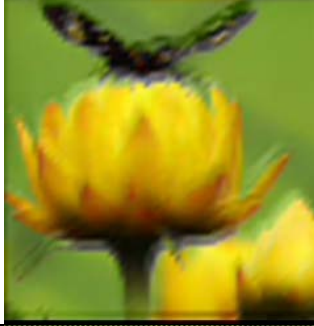
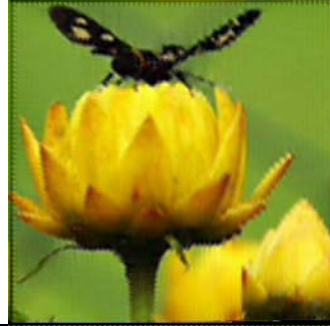

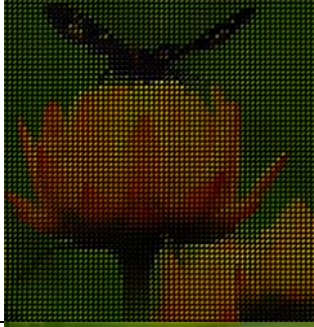



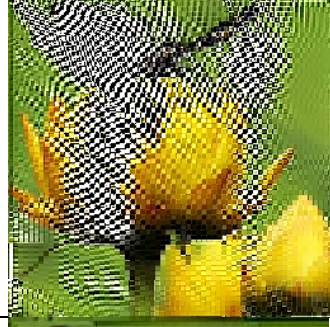








Figure 4.4: (a) Sample 2 HR image (b) (c) (d) (e) LR images with random transformation



Table 4.2: Comparison of different methods based on quality metrics for sample 2 image

Algorithms	Vandewalle	Marcel	Keren
<b>Interpolation</b>			
<b>Papoulis Gerchberg</b>			
<b>Iterated Back Projection (IBP)</b>			
<b>Robust Super Resolution</b>			
<b>Projection onto Convex Sets (POCS)</b>			

In above figure, figure 4.4 (a) is the sample HR image of dimension  $256 \times 256$ . Figures (b), (c), (d) and (e) are the LR images with random rotation and translation applied. Dimension of each LR image is reduced by factor 4. All the LR images of figure 4.4 are subjected to all three motion estimation algorithms and are reconstructed by all five reconstruction algorithms for each registration. Thus it helped to compare all possible combinations registration algorithms and reconstruction algorithm through the output images and corresponding MSE and PSNR values.

Table 4.3: PSNR values for table 4.2

<b>Reconstruction Method/Registration Method</b>	<b>Vandewalle</b>	<b>Marcel</b>	<b>Keren</b>
Interpolation	29.16	28.2	30.21
Papoulis Gerchberg	26.48	24.53	26.37
Iterated Back Projection	28.6	28.5	27.31
Robust Super Resolution	28.51	28.94	28.48
POCS	28.81	26.59	29.03

Above table shows the corresponding values of PSNR for reconstructed images of table 4.2 through different registration and reconstruction algorithms. The combination of Keren algorithm and POCS algorithm has the highest PSNR which is the best result among all in this experiment.

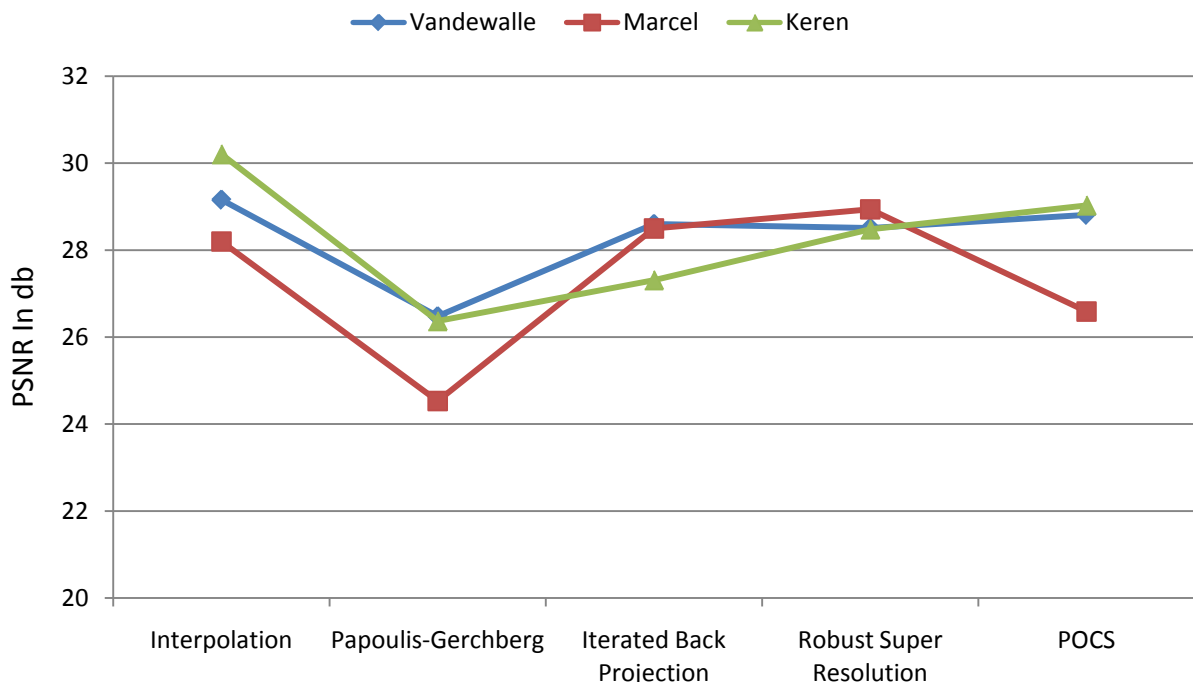


Figure 4.5: Plot of table 5.3

Figure 4.4 is the plot of data tabulated on table 4.3. From this plot, it is easier to estimate the best reconstruction algorithm for particular registration. For the Interpolation algorithm, Keren registration is best suited (PSNR = 30.21 db). Similarly for Iterated Back Projection and Robust SR algorithms, Marcel registration shows best result.

### Example 3

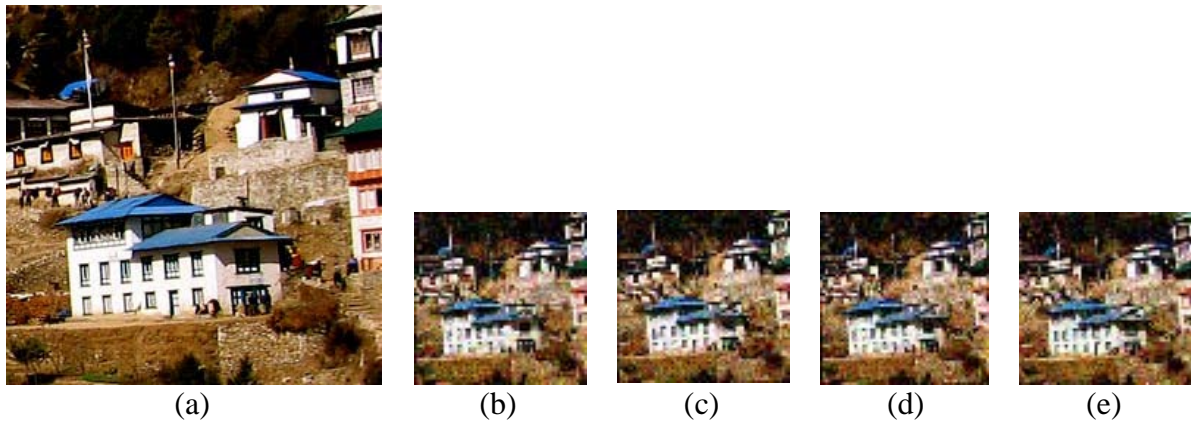


Figure 4.6: (a) Sample HR image (b) 10 db (c) 20 db (d) 30 db (e) 40 db LR images with random transformation

Example 3 images, (a) sample image 3 HR image with  $256 \times 256$  dimension. Image (b), (c), (d) and (e) are images with different level of added Gaussian noises.

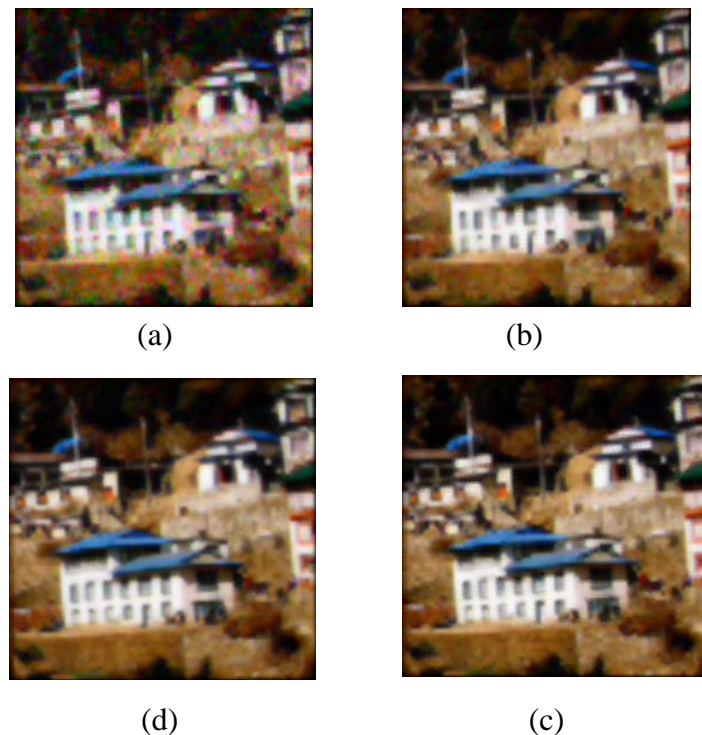


Figure 4.7: Reconstructed Images using POCS algorithm (a) 10 db (b) 20 db (c) 30 db (d) 40 db noise

Images with different noise level are recovered using POCS algorithm with Keren registration. No any filtering is implemented in above results.

Table 4.4: MSE and PSNR values for different noise level

<b>Error/Noise</b>	<b>10 db</b>	<b>20 db</b>	<b>30 db</b>	<b>40 db</b>
MSE	103.348	92.28	94.25	94.98
PSNR	27.99	28.47	28.38	28.35

Above table shows the MSE and PSNR values of image 3 under different Gaussian noise level. Using POCS algorithm image with 20 db has least MSE. Different other algorithms can also be used to recover the image.

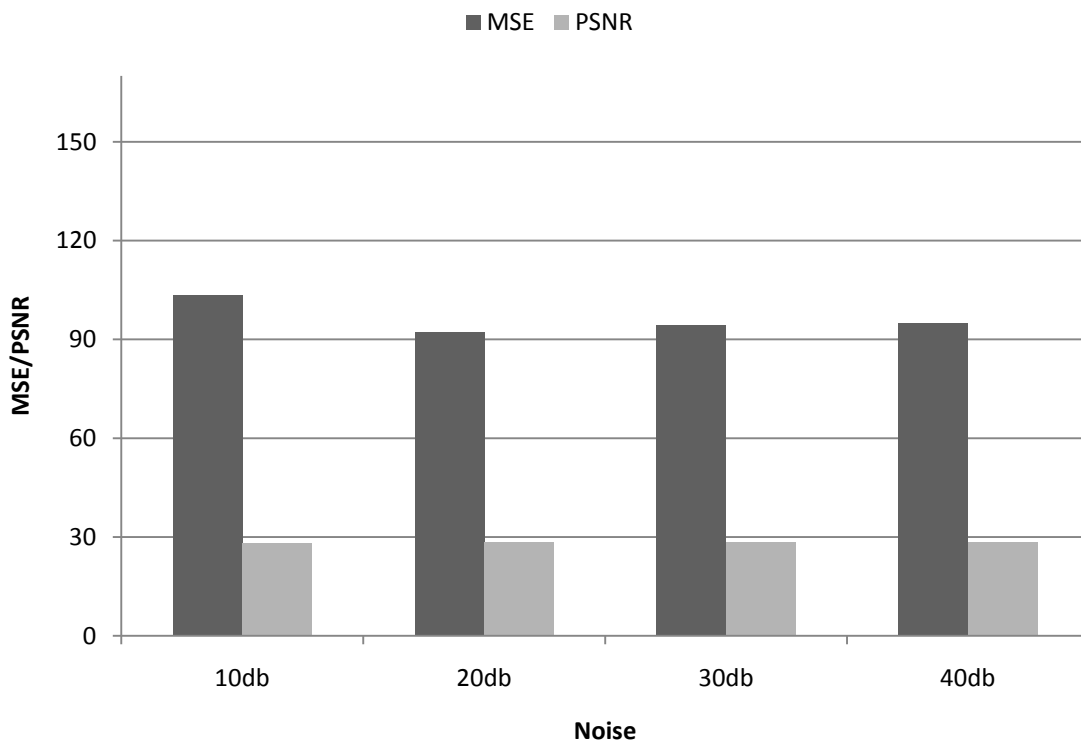


Figure 4.8: Bar graph of noisy image using Keren motion estimation reconstructed through POCS

Different noise levels are added to generate LR image and corresponding LR images with noise is applied to Keren registration algorithm to estimate the transformation parameters then HR image was constructed using POCS algorithm. The bar graph shows the corresponding errors for different level of noises. However the MSE was different for different level of noises, the PSNR remained almost constant.

Example 4


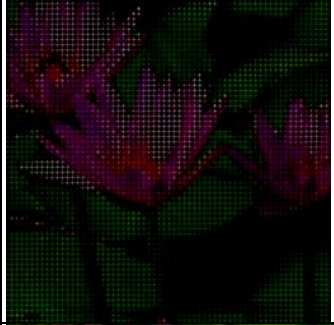
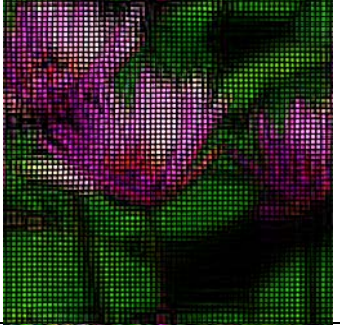







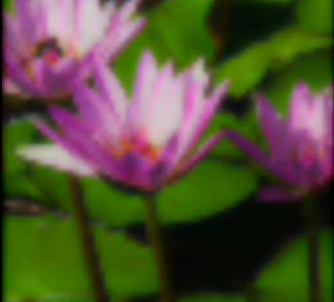



Figure 4.9: Original and transformed images (a) HR image and down sampled with transformation (b)  $1^{\circ}$ , (2.13, 3.92) pix (c)  $2^{\circ}$ , (4.67, 6.71) pix (d)  $5^{\circ}$ , (9.87, 1.39) pix LR images (e)  $10^{\circ}$ , (6.59, 8.83) pix LR images

In above figure, figure (a) is the sample HR image of dimension  $256 \times 256$ . Figures (b), (c), (d) and (e) are the LR images with different rotation and translation applied. Dimension of each LR image is reduced by factor 4. Blur and noise is not add to each LR image. The LR images are rotated with  $1^{\circ}, 2^{\circ}, 5^{\circ}, 10^{\circ}$  using these LR image all reconstruction algorithm is applied and their corresponding PSNR value are observed.

Table 4.5: Comparison of results obtained by Median and Weiner filtering methods for figure 4.9

Algorithms	Reconstructed image	Median filtered image	Weiner filtered image
Interpolation			

<p><b>Papoulis Gerchberg</b></p>			
<p><b>Iterated Back Projection (IBP)</b></p>			
<p><b>Robust Super Resolution</b></p>			
<p><b>Projection onto Convex Sets (POCS)</b></p>			

All the LR images of figure 4.9 are subjected to Keren motion estimation algorithm and are reconstructed by all five reconstruction algorithms. The table above shows the reconstructed image and the resulting output image after applying Median and Weiner filtering. The high degree rotation of LR images results poor quality output after reconstruction. However, the POCS method of reconstruction shows slightly better result after applying Median filter.

Table 4.6: PSNR values for the results obtained in Table 4.5

Reconstruction Method	Median filter	Weiner filter
Interpolation	27.87	27.91
Papoulis Gerchberg	25.23	26.17
Iterated Back Projection	27.52	27.69
Robust Super Resolution	27.66	27.61
POCS	28.1	28.12

Above table shows the corresponding values of PSNR for reconstructed images and the Median and Weiner filtered images of table 4.5 through Keren registration and different reconstruction algorithms. Nearly both filter with all algorithm shows same error values. PSNR value obtained in table 4.6 is less because of slightly large degree in rotation and large subpixel shift of LR ima

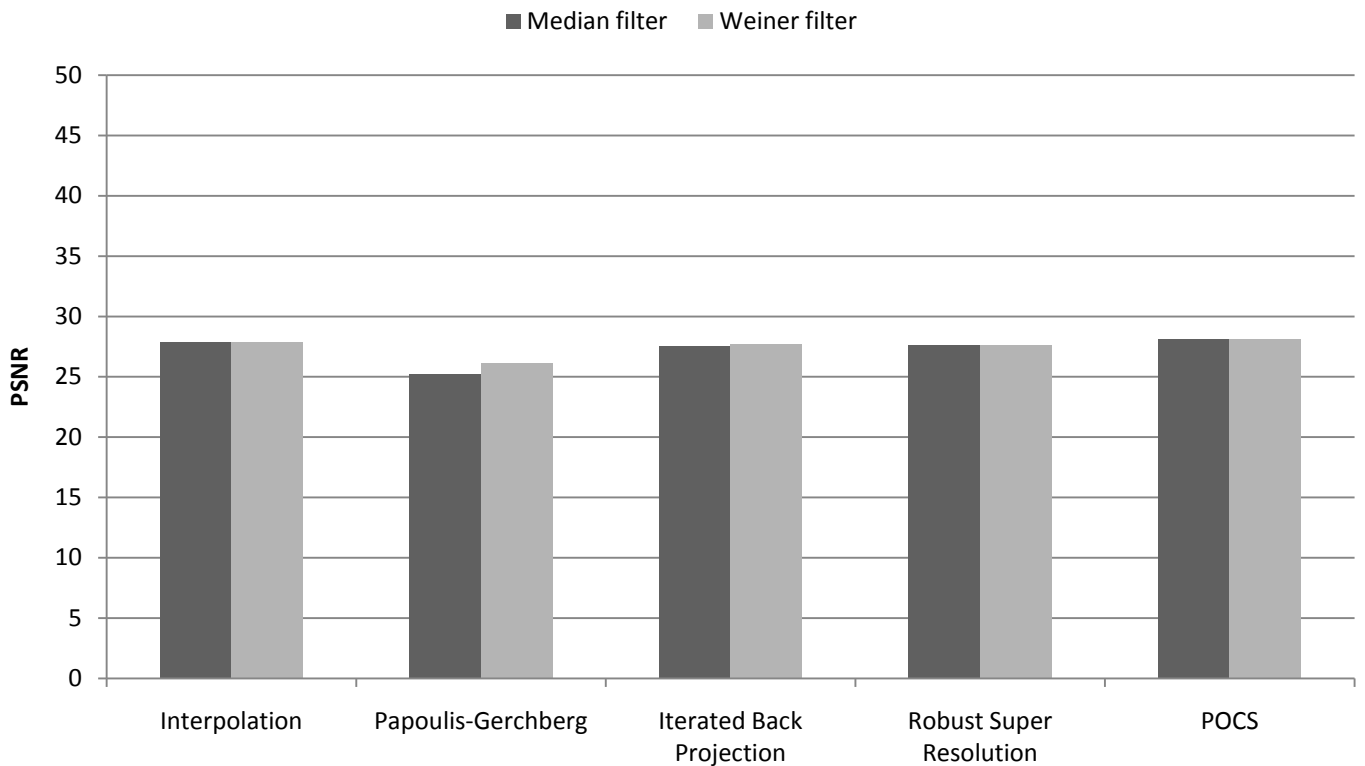


Figure 4.10: Bar graph of table 4.6

Figure 4.9 represents the table 4.6 in bar graph. From the bar graph shows Papoulis-Gerchberg algorithm has the slightly more error compared to others. Median filter and the Weiner filter have nearly equal error value can be observed .

Example 5

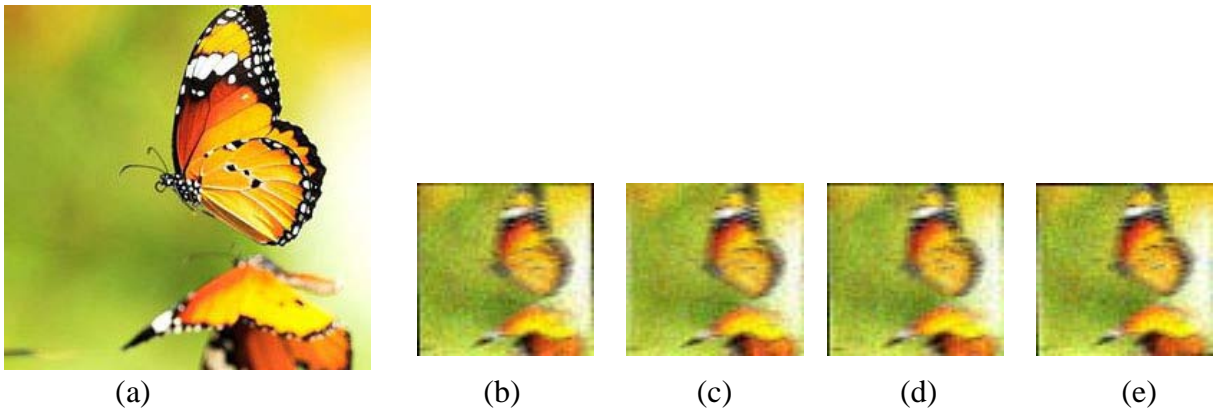
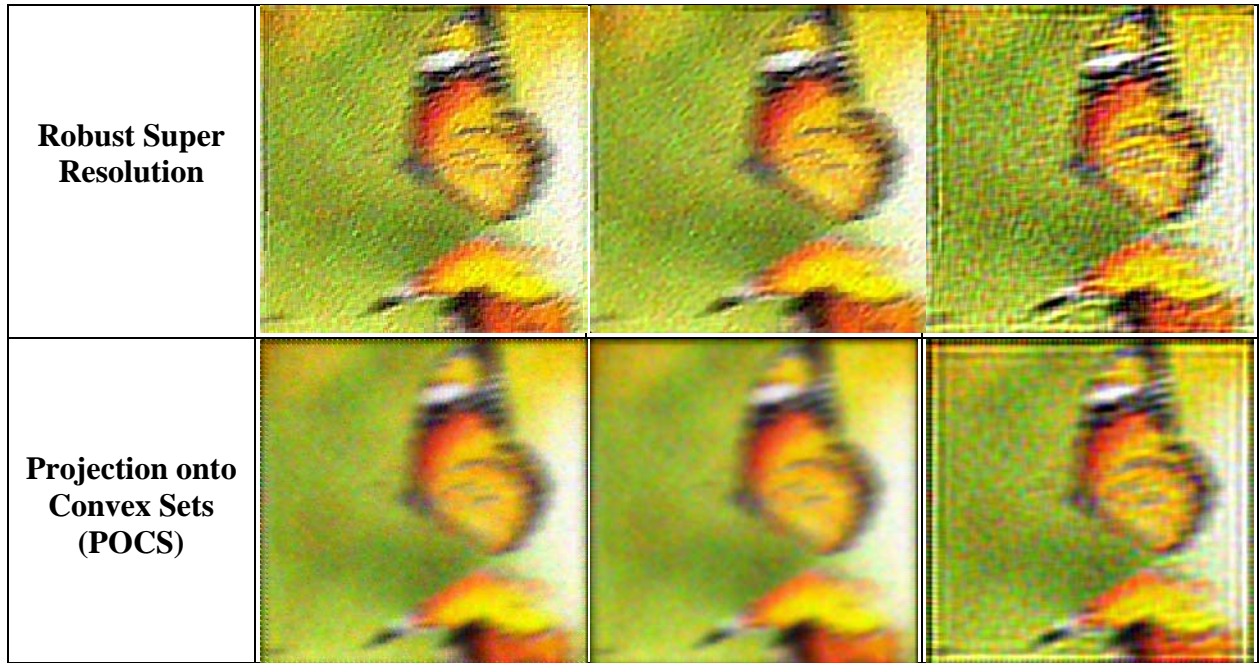


Figure 4.11: (a) Sample 4 HR image (b) (c) (d) (e) LR images with random transformation with motion blur and 10 db noise

Table 4.7: Comparison of results obtained by Median and Weiner filtering methods for figure 4.11

Algorithms	Reconstructed Image	Median Filtered Image	Weiner Filtered Image
Interpolation			
Papoulis Gerchberg			
Iterated Back Projection (IBP)			





All the LR images of figure 4.10 are subjected to Keren motion estimation algorithms and are reconstructed by all five reconstruction algorithms. The table above shows the reconstructed image and the resulting output image after applying Median and Weiner filter. The median filtered output images are better than Weiner filtered output images.

Table 4.8: PSNR values for the results obtained in table 4.7

<b>Reconstruction Method</b>	<b>Median filter</b>	<b>Weiner filter</b>
Interpolation	28.8	27.22
Papoulis Gerchberg	25.89	25.89
Iterated Back Projection	28.6	28.5
Robust Super Resolution	28.34	27.24
POCS	28.52	27.19

Above table shows the corresponding values of PSNR for reconstructed image and the Median and Weiner filter images of table 4.7. Keren motion estimation and different reconstruction algorithms are implemented for this. Nealy both filter shows same result with all algorithm except the Papulis-Gerchberg algorithm.

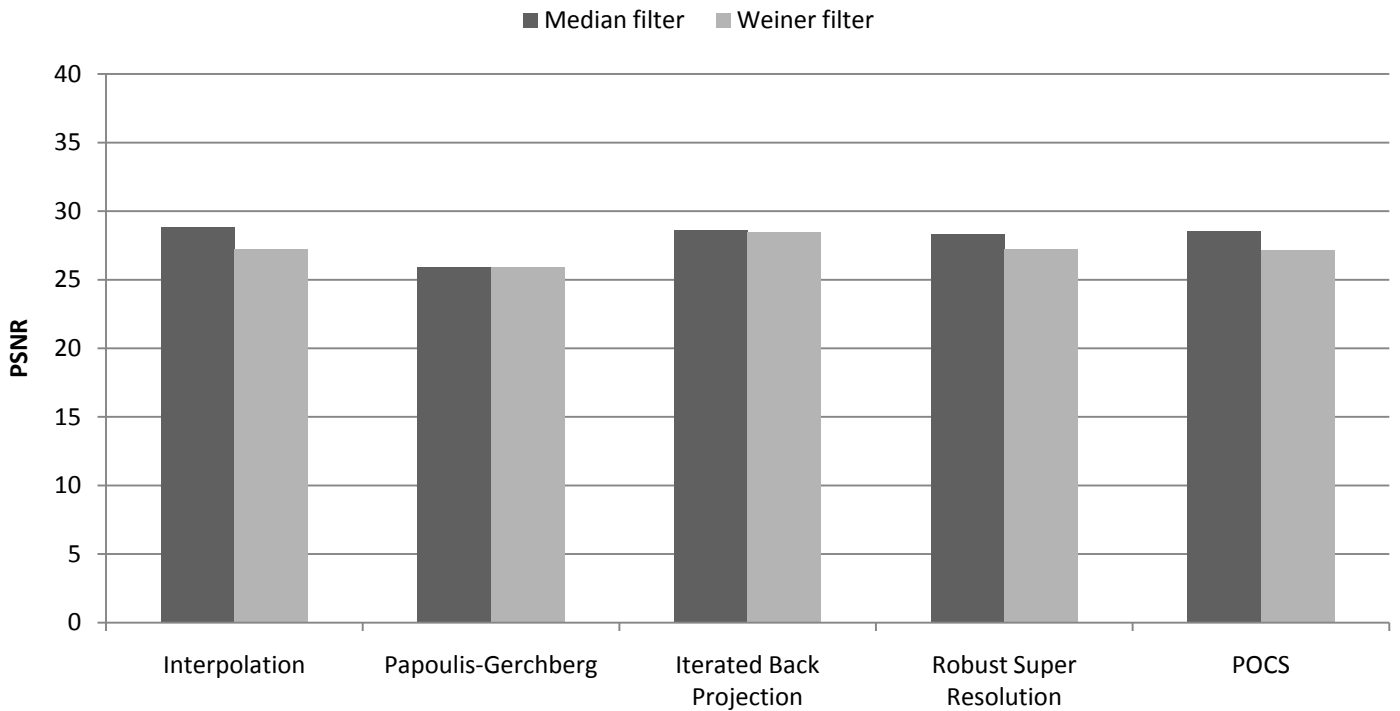


Figure 4.12: Bar graph of table 4.8

Figure 4.11 represents the table 4.8 in bar graph. From the bar graph it is observed that Papoulis Gerchberg algorithm has the more error compared to others. Median filter has better output than the Weiner filter.

#### Example 6

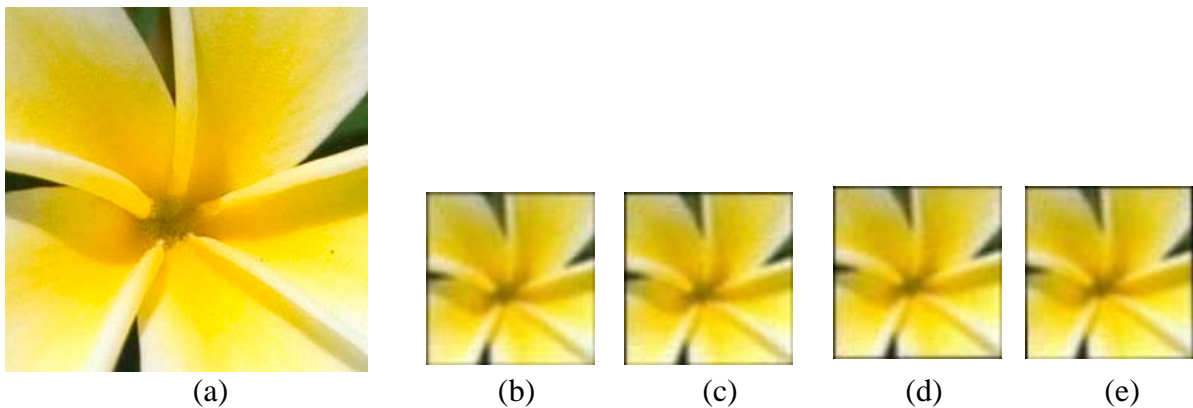



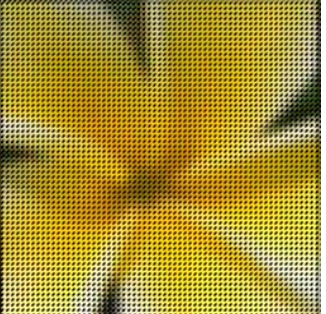

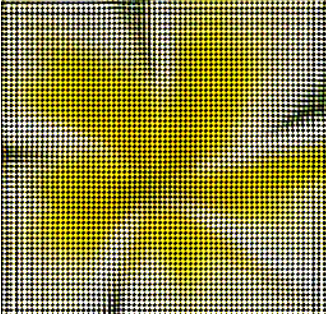


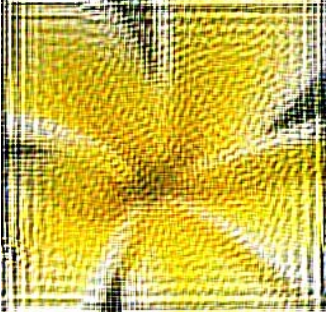


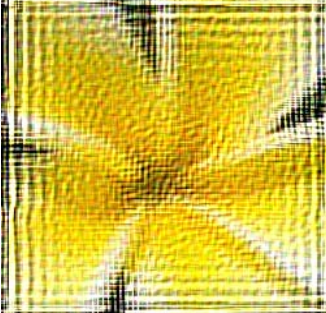





Figure 4.13: (a) Sample 5 HR image (b) (c) (d) (e) LR images with random transformation with average blur and 20 db noise

In above figure, figure (a) is the sample HR image of dimension  $256 \times 256$ . Figures (b), (c), (d) and (e) are the LR images with random rotation and translation applied. Dimension of each LR image is reduced by factor 4. Average blur and 20 db noise is add to each LR image.

Table 4.9: Comparison of results obtained by Median and Wiener filtering methods for figure 4.13

Algorithms	Reconstructed image	Median Filtered Image	Weiner Filtered Image
Interpolation			
Papoulis Gerchberg			
Iterated Back Projection (IBP)			
Robust Super Resolution			
Projection onto Convex Sets (POCS)			

All the LR images of figure 4.13 are subjected to Keren motion estimation algorithms and are reconstructed by all five reconstruction algorithms. The table above shows the reconstructed image and image after applying Median and Weiner filtering. The median filtered output images are better than Weiner filtered output images.

Table 4.10: PSNR values for the results obtained in table 4.9

<b>Reconstruction Method</b>	<b>Median filter</b>	<b>Weiner filter</b>
Interpolation	31.02	28.15
Papoulis Gerchberg	26.99	27.19
Iterated Back Projection	30.12	27.79
Robust Super Resolution	30.92	27.91
POCS	30.55	28.22

Above table shows the corresponding values of PSNR for reconstructed images and the Median and Weiner filter images of table 4.9 through Keren registration and different reconstruction algorithms. Nearly both filter with all algorithm shows same result except the Papulis Gerchberg algorithm. Adding average blur LR images are better reconstructed than motion blur LR images giving more PSNR values than table 4.7.

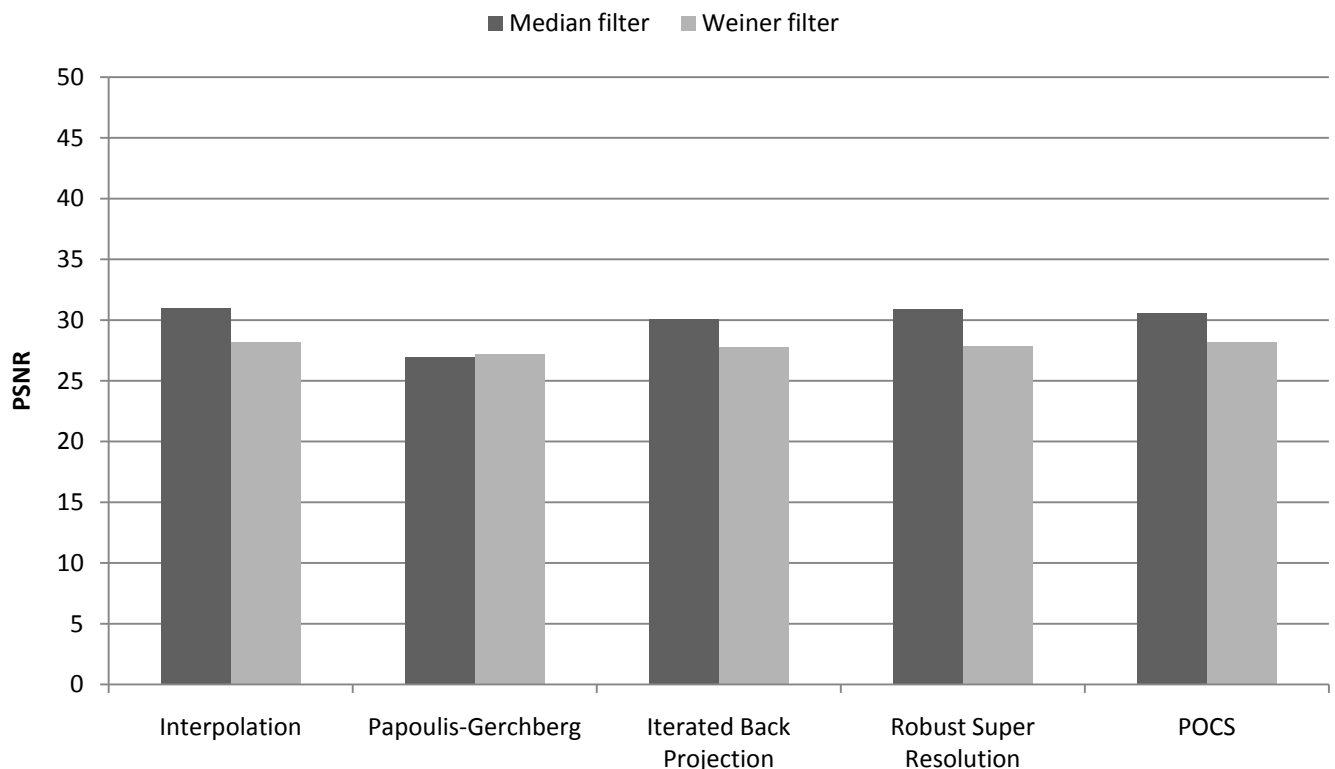


Figure 4.14: Bar graph of table 4.10

Figure 4.14 represents the table 4.10 in bar graph. From the bar graph it is observed that Papoulis Gerchberg algorithm has the more error compared to others. Median filter has better output than the Weiner filter. Interpolation and Robust super resolution have nearly equal PSNR values.

Example 7



Figure 4.15: (a) Sample 5 HR image (b) (c) (d) (e) LR images with random transformation with average blur and 20 db noise

In above figure, figure (a) is the sample HR image of dimension  $256 \times 256$ . Figures (b), (c), (d) (e) and (f) are the LR images with random rotation and translation with Gaussian blur and 10db noise applied. Dimension of each LR image is reduced by factor 4.

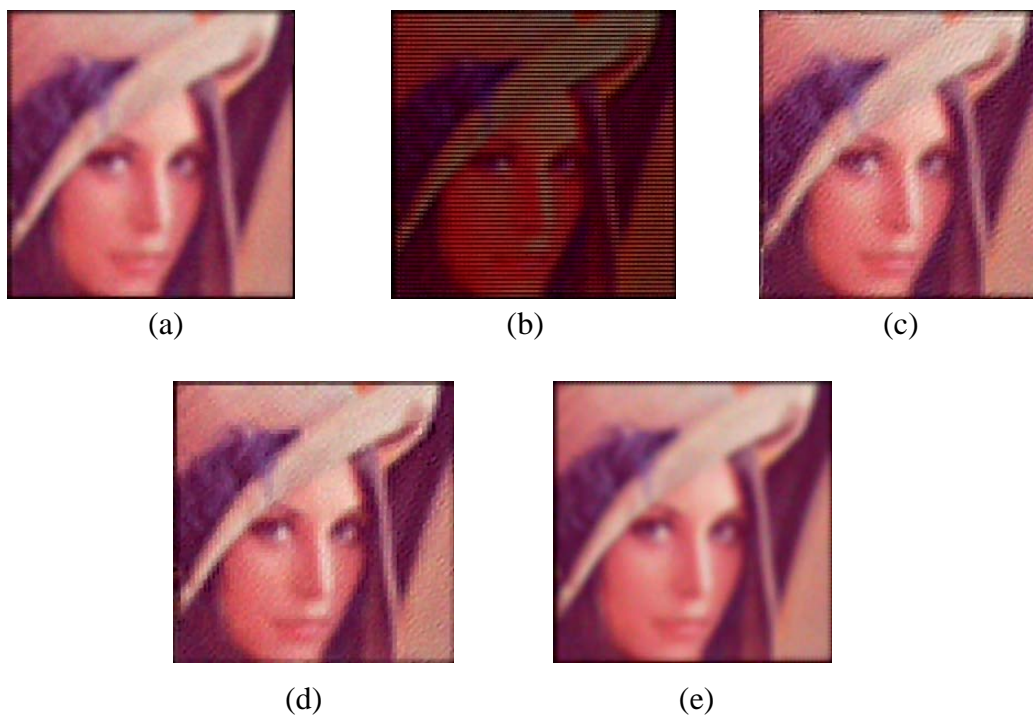


Figure 4.16: Reconstructed Images (a) Interpolation (b) Papoulis Gerchberg (c) Iterated Back Projection (d) Robust Super Resolution (e) POCS

The figure above shows the reconstructed output images from different algorithms after applying Median filter. The five low resolution images shown in figure 4.14 are used for reconstruction. The results obtained by interpolation, IBP, Robust SR and POCS methods are nearly similar. Papoulis Gerchberg method shows poor image quality than others.

Table 4.11: PSNR values for the results obtained by Median and Weiner filtering

Reconstruction Algorithm	Metrics	Number of Low Resolution images					
		Four	Five	Six	Seven	Eight	Nine
Interpolation	MSE	69.38	69.47	68.65	69.71	68.19	69.96
	PSNR	29.72	29.71	29.76	29.7	29.79	29.68
Papoulis Gerchberg	MSE	72.57	151.17	169.94	124.1	123.63	107.95
	PSNR	29.52	24.13	25.83	24.63	24.64	27.8
Iterated Back Projection	MSE	70.31	127.42	75.19	127.25	73.56	127.54
	PSNR	29.66	27.08	29.37	27.08	29.46	27.07
Robust Super Resolution	MSE	70.28	69.15	66.76	71.07	119.31	110.7
	PSNR	29.66	29.73	29.89	29.61	27.36	27.69
POCS	MSE	74.95	71.38	70.76	72.51	73.27	71.41
	PSNR	29.38	29.6	29.63	29.53	29.48	29.59

Above table 4.11 shows the corresponding values of MSE and PSNR for reconstructed images after applying Median filter. The different number of low resolution are simulated each image added with gaussian blur and 20db noise. Using these different low resolution image the reconstruction is done through keren registration and different reconstruction algorithms. From the data shown in table the different variation in the quality of output images due to the effect of increasing the number of low resolution image .

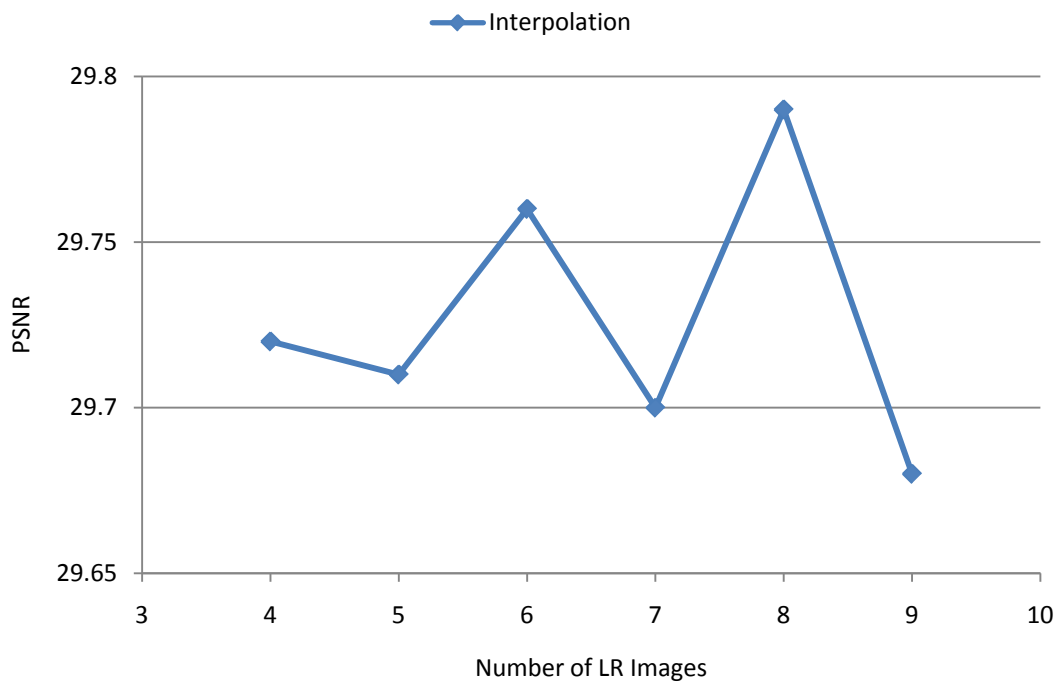
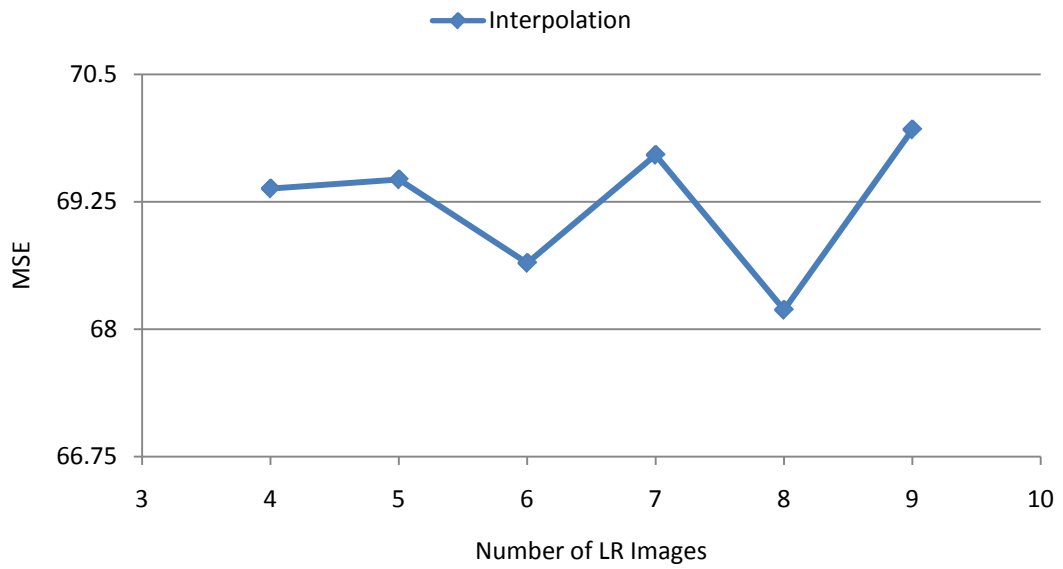


Figure 4.17: Effect of image quality for Interpolation method

The interpolation method get some better quality in the reconstruted image. This algorithm have nearly same MSE and PSNR value for the increase number of low resolution images. The error values are less for the interpolation method than other reconstruction methods.

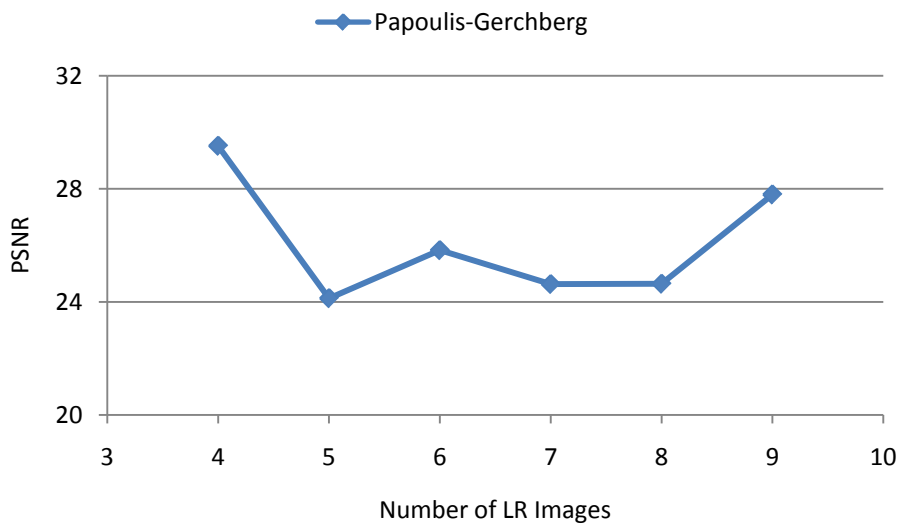
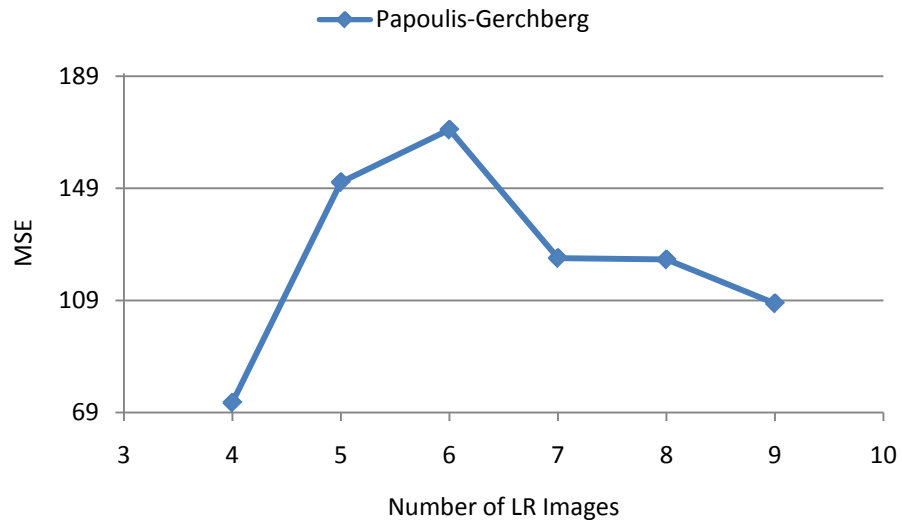


Figure 4.18: Effect of image quality for Papoulis Gerchberg method

The figure 4.18 shows the plot of Papoulis Gerchberg method of reconstruction showing the values of quality metrics MSE and PSNR. The error values are decreasing slowly as the number of low resolution images increases. Still the result is poor compared to interpolation.



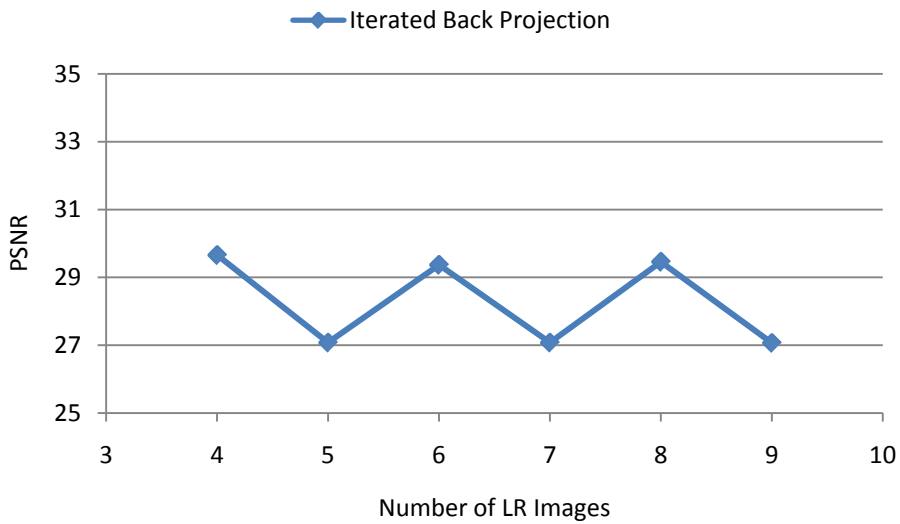
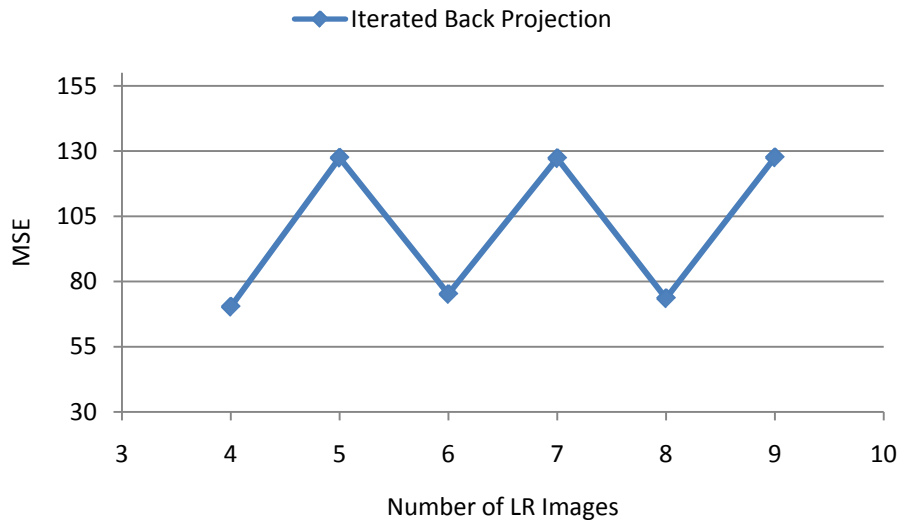


Figure 4.19: Effect of image quality for IBP method

The figure 4.19 shows the plot of Iterated Back Projection (IBP) method of reconstruction showing the values of quality metrics MSE and PSNR. The error values are not changing linearly as the number of low resolution images increases. Still the result is better compared to Papoulis Gerchberg method but not good like interpolation method.

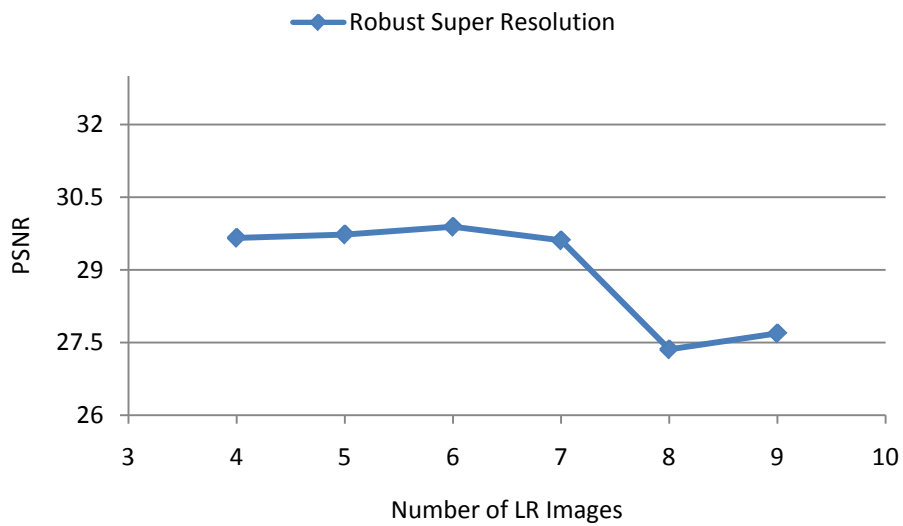
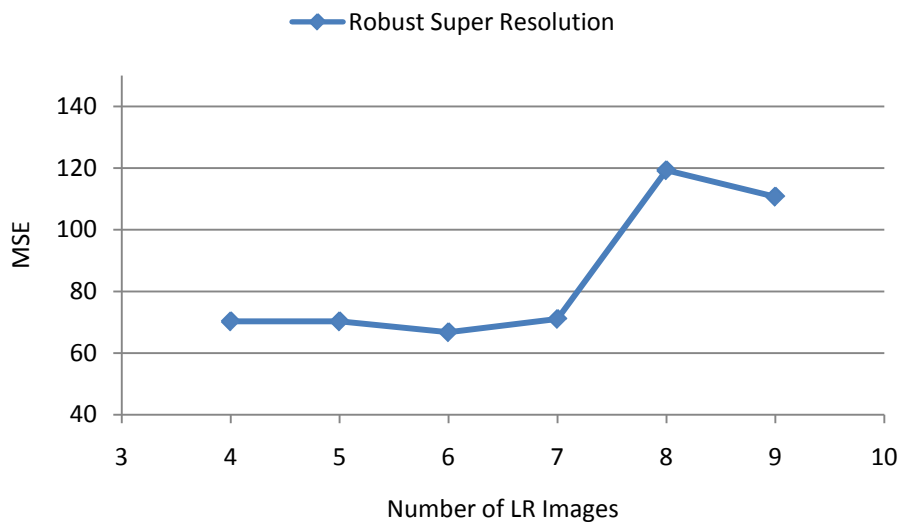


Figure 4.20: Effect of image quality for Robust SR method

The figure 4.20 shows the plot of Robust Super Resolution method of reconstruction showing the values of quality metrics MSE and PSNR. This method doesnot shows any improvement with the increase number of low resolution images. Increasing in the number of low resolution images, this methods show more error due to lack of new information addition to the images.

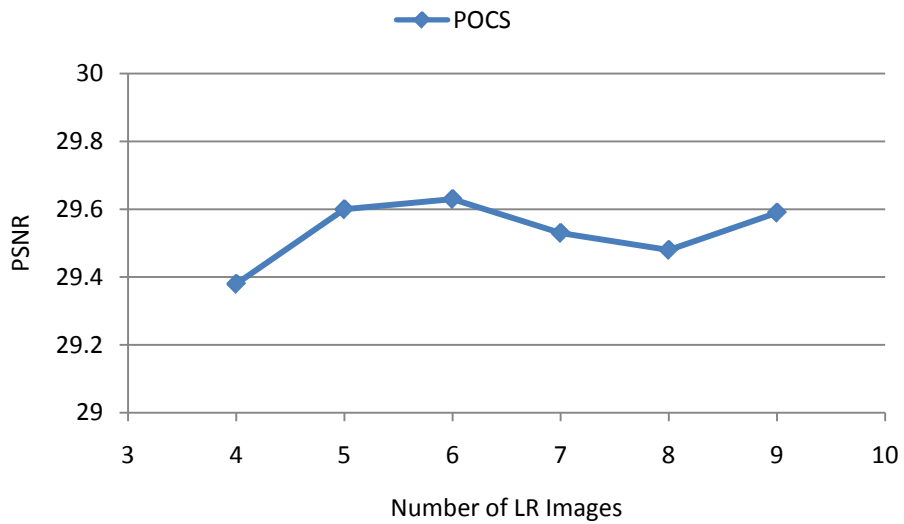
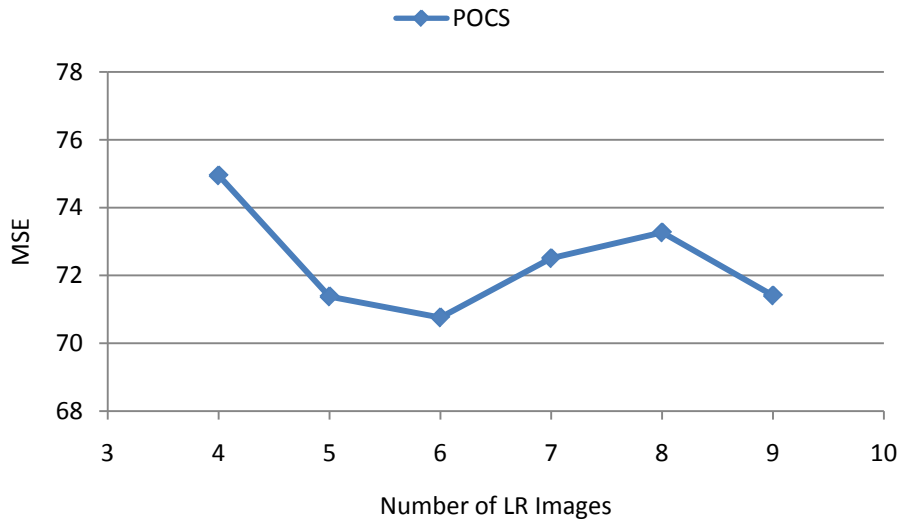


Figure 4.21: Effect of image quality for POCS method

The figure 4.21 shows the plot of Projection onto Convex Sets(POCS) method of reconstruction showing the values of quality metrics MSE and PSNR. Among the five reconstruction method this method shows slightly better quality in output image. The error values are slowly decreasing as the number of low resolution images increases.

## 4.2 Test Based on Real Images

After the multiple experiment with the simulated images, the real images are tested and analyze their quality of images after reconstruction by various algorithm. 12 different dataset for the real low resolution images are taken from the internet and tested. Detail information about the real images are mention in Appendix section. Some of tested results are shown below.

### 4.2.1 Experiment Results

Since only the size of the low resolution image are known and the other parameters and other factors like amount of sub pixel shifting and rotation, actual content of blur and noise are unknown. The all possible method of reconstruction are performed and compare the results obtained.




Example 1















Figure 4.22: Sample 1 Real LR images

Above figure show five  $100 \times 100$  size real low resolution images of the same scene with unknown transformation and the actual content of blur and noise.

Table 4.12: Comparison of different methods based on quality metrics for figure 4.22

Algorithms	Vandewalle	Marcel	Keren
Interpolation			

<p><b>Papoulis Gerchberg</b></p>			
<p><b>Iterated Back Projection (IBP)</b></p>			
<p><b>Robust Super Resolution</b></p>			
<p><b>Projection onto Convex Sets (POCS)</b></p>			

All the LR images of figure 4.22 are subjected to Vandewalle, Marcel and Keren motion estimation algorithms and are reconstructed by all five reconstruction algorithms. The table above shows the reconstructed image and the resulting output image of size 400×400 size after applying Median filter. Though the transformation and nature of blur and noise content present is unknown among five reconstruction method, POCS method outputs good results and Papoulis Gerchberg method low quality images. The reconstruction time for Robust Super Resolution method is higher than others method.

Example 2

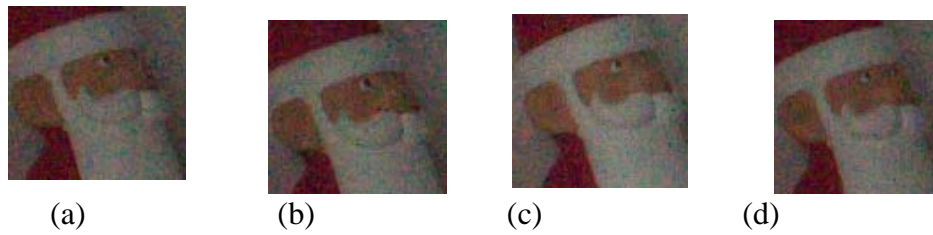








Figure 4.23: Sample 2 Real LR images

Above figure show the four  $100 \times 100$  size real low resolution images of the same scene with unknown transformation and the actual content of blur and noise.

Table 4.13: Comparison of different methods based on quality metrics for figure 4.23

Algorithms	Vandewalle	Marcel	Keren
<b>Interpolation</b>			
<b>Papoulis Gerchberg</b>			
<b>Iterated Back Projection (IBP)</b>			

<p><b>Robust Super Resolution</b></p>			
<p><b>Projection onto Convex Sets (POCS)</b></p>			

All the LR images of figure 4.23 are subjected to Vandewalle, Marcel and Keren motion estimation algorithms and are reconstructed by all five reconstruction algorithms finally median filtered. The table above shows the reconstructed image and the resulting output image after applying Median filter. Though the transformation and nature of blur and noise content present is unknown among five reconstruction method. Iterated Back Projection, Robust Super Resolution, POCS methods have better quality images than Interpolation and Papoulis Gerchberg method.

### Example 3

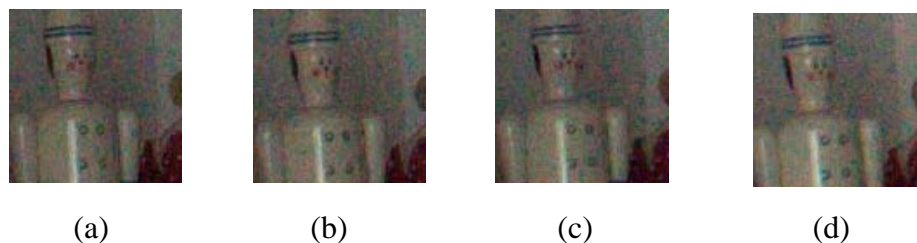







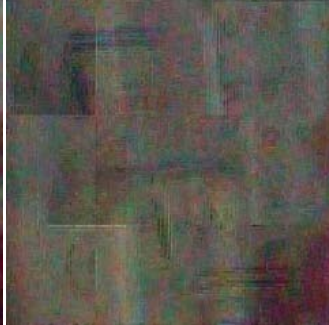









Figure 4.24: Sample 3 Real LR images

Above figure show the four  $100 \times 100$  size real low resolution images of the same scene with unknown transformation and the actual content of blur and noise.

Table 4.14: Comparison of different methods based on quality metrics for figure 4.24

Algorithms	Vandewalle	Marcel	Keren
<b>Interpolation</b>			
<b>Papoulis Gerchberg</b>			
<b>Iterated Back Projection (IBP)</b>			
<b>Robust Super Resolution</b>			
<b>Projection onto Convex Sets (POCS)</b>			



All the LR images of figure 4.24 are subjected to Vandewalle, Marcel and Keren motion estimation algorithms and are reconstructed by all five reconstruction algorithms finally median filtered. The table above shows the reconstructed image and the resulting output image after applying Median filter. Though the transformation and nature of blur and noise content present is unknown among five reconstruction method, Keren motion estimation algorithm and POCS method outputs good results than others methods.

Example 4

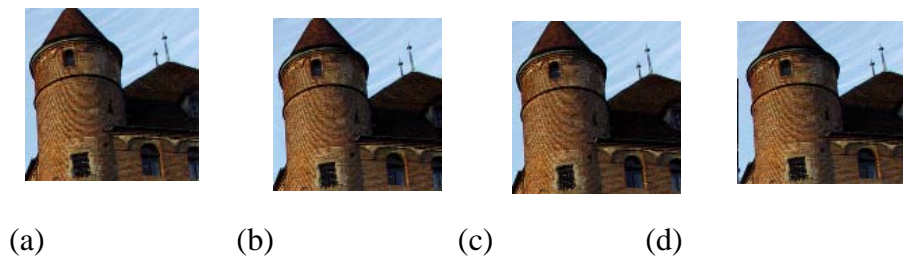


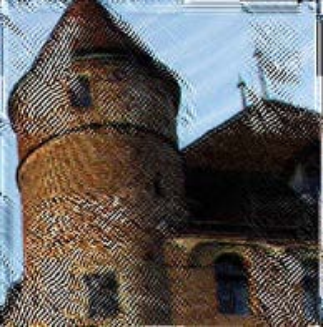




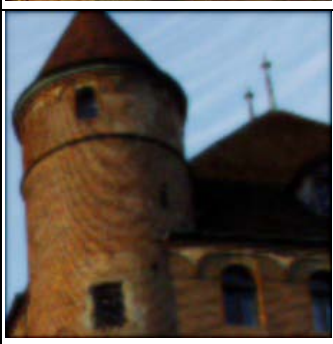



Figure 4.25: Sample 4 Real LR images

Above figure show four 100×100 size real low resolution images of the same seen with unknown transformation and the actual content of blur and noise.

Table 4.15: Comparison of different methods based on quality metrics for figure 4.25

Algorithms	Vandewalle	Marcel	Keren
Interpolation			
Papoulis Gerchberg			

<p><b>Iterated Back Projection (IBP)</b></p>			
<p><b>Robust Super Resolution</b></p>			
<p><b>Projection onto Convex Sets (POCS)</b></p>			

All the LR images of figure 4.25 are subjected to Vandewalle, Marcel and Keren motion estimation algorithms and are reconstructed by all five reconstruction algorithms and finally Median filtered. The table above shows the reconstructed image and the resulting output image after applying Median filter. Marcel motion estimation algorithm and Papoulis Gerchberg method outputs worst results. Robust Super Resolution method using Vandewalle algorithm results shows poor quality image.

### 4.3 Discussion

Motion Estimation is a crucial step in Super resolution methodology. During this study, three motion estimation methods are examined. Two of them are frequency domain methods and remaining one is spatial domain techniques. The spatial domain techniques is more stable than the frequency domain techniques. The reason for this is the spatial domain techniques are computationally efficient and give accurate results. Vandewalle et al, Marcel et al and Keren et al algorithms are studied in this thesis. The examination shows that Vandewalle et al and Marcel et al algorithm does not give better result in case of presence of blur and noise and are less efficient than Keren et al algorithm. As a result in most of the cases Keren et al method is used for both synthetic and real images.

In addition, the restoration techniques namely Interpolation, Papoulis Gerchberg, Iterated Back Projection (IBP) and Projection onto Convex sets (POCS) combine all the information available from motion estimation algorithm to recover HR images are examined. Among these only interpolation is the single frame techniques and remaining four are multi frame techniques. The obtained results shows single frame techniques work very effectively and give good results without any concern about the weight of the computational load.

The accurate and precise sub pixel motion information, knowledge of imaging system degradation during image acquisition, actual content of noise and blur in the real images are the important factors that affect the performance of all of these techniques. Similarly, the restoration method must include well defined priori information. The results obtained by these techniques are examined based on the quality metrics.

The effectiveness of the motion estimation algorithm is vital to obtain the efficient result from the SR methods. Interpolation and POCS method use the information of all images very efficiently and force the HR image to be bounded by range of pixels determined from LR images. If there is registration error, the placement of false pixel locations may occur. These two methods turned out to be the most successful method in this study.

Iterative Back Projection (IBP) method is another efficient method found during this study. This method eliminate various errors at the back projection stage result than remaining three methods. IBP equate the solution by back projecting the information from new LR images at each iteration and smoothes the reconstruction algorithm. Robust

SR method computationally less efficient because this method takes more time for reconstruction than other techniques. The visual quality of output image by Papoulis Gerchberg method is poor among the five methods. The improvement of images quality is clear especially for the IBP and POCS techniques.

Transformation parameters in the LR images affect largely in the quality of reconstruction. The experiment is performed up to 0.8 sub pixel shift in horizontal and vertical axis and with rotation maximum of  $1^\circ$ ,  $2^\circ$ ,  $5^\circ$ ,  $10^\circ$ . Larger the value of transformation parameters lesser the quality of reconstruction. Additionally noise and blur is the another problem for all SR reconstruction methods. The reconstruction process does not take directly into account blurring and noise of input LR images. It may cause loss of detail that is need at the stage of reconstruction. Similarly, experiment is perform for both different types of blur and noisy images. The content of blur and noise is randomly chosen for the synthetic images where as the amount of contents is unknown for the real images. Median filter and Weiner filter is applied to the images obtained by different reconstruction methods in next stage. The study shows that the Median filter yields better results than Weiner filter for images obtained by POCS method. The number of LR images does not shows any strong affect in the solution in both case of using synthetic and real LR images.

A major problem is the lack of a suitable objective metric for the assessment of the quality of image restores by SR techniques. Mean Square Error(MSE) and peak signal to noise ratio(PSNR) are widely used in image processing. These two metrics are used to evaluate the synthetic images. However, the reference image is not known in real situation. MSE error based measurements are not able to describe the improvement in the visual quality of image. Therefore only visual assessment is performed in the real images for the measurement of reconstruction quality.

**CHAPTER 5**  
**CONCLUSION AND RECOMMENDATION**

## 5. Conclusion and Recommendation

### 5.1 Conclusion

Super resolution is the method of recovering low resolution images which has a wide range of application in image processing. Motion estimation algorithms and restoration techniques are the process of the super resolution. This research especially based on the study of effect of the motion estimation and the restoration methods by implementing some of the well known algorithms mentioned in literature and experimenting on them using both synthetic and real images. Further this study also focus on the deblurring and denoising the result obtained by those algorithms .

In this thesis, different super resolution reconstruction methods are examined by conducting experiment on multiple simulated and real images. The goal is to combine the information of multiple low resolution images and construct a single high resolution image. The problem is complex due to unknown point spread function of imaging device, varying imaging conditions and necessity of efficient motion estimation algorithm. All these parameters make the problem difficult with non unique solution.

The key to successful SR reconstruction lies in a robust and effective motion estimation algorithm. Misaligned images may cause loss of detail information instead of improving the resolution. For this case the single frame interpolation methods can be choose in the case if the images data set cannot be registered properly. Bicubic interpolation methods provide the desired requirements for image quality with computational speed. For multi frame reconstruction methods Iterated Back Projection (IBP) and POCS methods can be selected for the successful image registration. These methods yields better results than the single frame method for different motion model, number of LR images and up sampling factor.

In practical cases, the blurring and noise is often unknown. The performance of restoration methods degrade in the quality of reconstruction. This is due to critical dependence of motion estimation algorithm. So another stage is added to enhance the image quality. In this case the image filtering is by Median and Weiner filter to remove the blur and noise present on LR images. If the noise and blur is above the certain threshold level it can be better to use single frame interpolation method.

Finally, the obtained result by different SR methods are compared on the basis of quality metrics. For this, mean Square Error(MSE) and peak signal to noise ratio(PSNR) value are calculated for synthetic image and analyze the results. Only visual assessment of image quality improvement is done in the case of real images.

## **5.2 Limitation**

In this thesis, the performance analysis and testing of three registration algorithm and five reconstruction method are performed in more synthetically generated images. However, 12 the real images are tested. Since, due to the unavailability of sufficient number of real images analysis results are based on simulated images. During this thesis work, the global translation motion in the LR images is assumed. It can be modify and study on local translation motion.

Also in this thesis observations models covers only Average, Gaussian and Motion blur and additive white Gaussian noise. Median filter and Weiner filter are only the deblurring and denoising techniques implemented. Some of the outputs images are of not good quality because of lack of more filtering methods.

## **5.3 Recommendation**

In this thesis, the comparative study are done only for three registration algorithm and five reconstruction method. These algorithm can be further compared with other super resolution algorithm for better performance study of them. Different types of other blur and noise can be added in the observation model.

Further enhancement of this work can be done by experiment with large number of real data set and analyze the performance of the motion estimation and SR reconstruction techniques in depth. Different deblurring and denoising techniques can be added to enhance the improvement in the quality of reconstruction.

## REFERENCES

- [1] R. Ramya, Dr. M. Senthil Murugan, "Comparative Study on Super Resolution Image Reconstruction Techniques," Volume : 3, Issue : 10 , Oct 2013 , ISSN - 2249-555X.
- [2] S. C. Park, M. K. Park, and M. G. Kang, "Super-resolution image reconstruction: A technical overview," *IEEE Signal Processing Magazine*, vol. 20, no. 3, pp. 21-36, May 2003.
- [3] B. L. ping, L. Q. hui, W. B. jian, Z. H. xin, "High Resolution Infraed Image Reconstruction Based on Image Sequence", *Infrared Technology*, vol. 24, no. 6, pp. 58-61, 2002.
- [4] Changh, Yeu Ngdy, Xiongym, "Super-resolution th rough neighbor embedding", *Proceedings of the IEEE C o mputer So ciety Conference on Computer Vision and Pattern Recognition*, 2004, pp. 275-282.
- [5] E.J. Cand`es and M.B. Wakin, "An introduction to compressive sampling". *IEEE Signal Processing Magazine*, 2008, pp. 21-30.
- [6] J. WRIGHT, T.HUANG, Y. MA, "Image super-resolution as sparse representation of raw," *IEEE Conference on Computer Vision and Pattern Recognition*, 2008, pp. 1-8.
- [7] Rhee, S.H. and Kang, M.G, "Discrete cosine transform based regularized high resolution image reconstruction algorithm" ,*SPIE Opt. Eng*, 38.1999.
- [8] L. Lucchese and G. M. Cortelazzo, "A noise-robust frequency domain technique for estimating planar roto-translations," *IEEE Transactions on Signal Processing*, vol. 48, no. 6, pp. 1769– 1786, 2000.
- [9] A. Maurya, R. Tiwari , " A Novel Method of Image Restoration by using Different Types of Filtering Techniques" *International Journal of Engineering Science and Innovative Technology (IJESIT)* Volume 3, Issue 4, July 2014.
- [10] P. Vandewalle, S. Sússtrunk and M. Vetterli, " A Frequency Domain Approach to Registration of Aliased Images with Application to Super-Resolution",



*EURASIP Journal on Applied Signal Processing*, Vol. 2006, pp. Article ID 71459, 14 pages, 2006.

- [11] B. Marcel, M. Briot, and R. Murrieta," Calcul de Translation et Rotation par la Transformation de Fourier", *Traitement du Signal*, vol. 14, no. 2, pp. 135-149, 1997.
- [12] D. Keren, S. Peleg, and R. Brada," Image sequence enhancement using sub-pixel displacement", *Proceedings IEEE Conference on Computer Vision and Pattern Recognition*, June 1988, pp. 742-746.
- [13] R.G.Krys," Cubic Convolution Interpolation for Digital Signal Processing", *IEEE Trans Acoust,Speech,and Signal Process*,vol.29,pp.1153-1160,1981.
- [14] Priyam Chatterjee, Sujata Mukherjee, Subhasis Chaudhuri, Guna Seetharaman, "Application of Papoulis-Gerchberg Method in Image Super-resolution and Inpainting".
- [15] A. Zomet, A. Rav-Acha, and S. Peleg," Robust Super-Resolution", *Proceedings international conference on computer vision and pattern recognition (CVPR)*, 2001.
- [16] S. Kumar, P. Kumar, M. Gupta, A. K. Nagawat , " Performance Comparison of Median and Wiener Filter in Image De-noising", *International Journal of Computer Applications* (0975 – 8887). Volume 12– No.4, November 2010. 27.

# Appendix A

## Methods Used

Different image registration algorithm and super resolution reconstruction methods used in this thesis work is tabulated below.

Table A.1: Image Registration Methods

S.N.	Methods
1	Vandewalle Algorithm
2	Marcel Algorithm
3	Keren Algorithm

Table A.2: Super Resolution Reconstruction Methods

S.N.	Methods
1	Interpolation
2	Papoulis Gerchberg
3	Iterated Back Projection (IBP)
4	Robust Super Resolution
5	Projection onto Convex Sets (POCS)

## Appendix B

Test Image 1



Figure B.1: Original and transformed images (a) HR image (b) down sampled, no transformation (c)  $0^\circ$ , (0.479, 0.911) pix (d)  $0.9^\circ$ , (0.737, 0.802) pix (e)  $1^\circ$ , (0.123, 1.019) pix LR images

Table B.1: List of different HR images using different registration and reconstruction algorithms

Algorithms	Vandewalle	Marcel	Keren
<b>Interpolation</b>			
<b>Papoulis Gerchberg</b>			
<b>Iterated Back Projection (IBP)</b>			
<b>Robust Super Resolution</b>			
<b>Projection onto Convex Sets (POCS)</b>			

Above figure B.1 shows original HR image and differently transformed LR images. These transformation parameters are entered manually and corresponding LR images are generated using MATLAB. Using different registration algorithm, different SR algorithms are implemented to test image 1 and above table B.1 shows all the results.

Table B.2: Manually entered transformation parameters

Rotation	Translation	
Angle (in degree)	x	y
0	0	0
0	0.479	0.911
0.9	0.737	0.802
1	0.123	1.019

For four LR images to generate four different parameters are entered manually. First image is not transformed so inputs are  $0^0$  and  $(0, 0)$  pixel shifts and other three are transformed using above table data.

Table B.3: MSE and PSNR of Test image 1 for different algorithms

Algorithms	Error	Vandewalle	Marcel	Keren
Interpolation	MSE	49.76	72.97	42.53
	PSNR	31.16	29.5	31.84
Papoulis Gerchberg	MSE	120.52	196.45	138.48
	PSNR	27.32	25.2	26.72
Iterated Back Projection	MSE	66.66	70.83	64.53
	PSNR	29.89	29.63	30.0344
Robust Super Resolution	MSE	61.84	73.64	57.79
	PSNR	30.22	29.46	30.51
POCS	MSE	54.4	100.18	50.79
	PSNR	30.77	28.12	31.07

Table B.3 shows the MSE and PSNR of Test image 1 for different motion estimation algorithm recovered with different SR reconstruction algorithms.

Test image 2



Figure B.2: Original and transformed images (a) HR image (b) down sampled, no transformation (c)  $0^\circ$ , (0.479, 0.911) pix (d)  $0.9^\circ$ , (0.737, 0.802) pix (e)  $1^\circ$ , (0.123, 1.019) pix LR images

Table B.4: List of different HR images using different registration and reconstruction algorithms

Algorithms	Vandewalle	Marcel	Keren
Interpolation			
Papoulis Gerchberg			
Iterated Back Projection (IBP)			
Robust Super Resolution			
Projection onto Convex Sets (POCS)			

Above figure shows original HR image and differently transformed LR images. These transformation parameters are entered manually and corresponding LR images are

generated using MATLAB. Using different registration algorithm, different SR algorithms are implemented to test image 2 and above table shows all the results.

Table B.5: Manually entered transformation parameters

Rotation	Translation	
Angle (in degree)	x	y
0	0	0
0	0.479	0.911
0.9	0.737	0.802
1	0.123	1.019

For four LR images to generate four different parameters are entered manually. First image is not transformed so inputs are  $0^0$  and (0, 0) pixel shifts and other three are transformed using above table data.

Table B.6: MSE and PSNR of Test image 2 for different algorithms

Algorithms	Error	Vandewalle	Marcel	Keren
Interpolation	MSE	60.16	83.28	46.99
	PSNR	30.34	28.93	31.41
Papoulis Gerchberg	MSE	124.44	234.28	144.46
	PSNR	27.18	24.43	26.53
Iterated Back Projection	MSE	100.65	81.96	122.28
	PSNR	28.1	28.99	27.26
Robust Super Resolution	MSE	76.55	80.03	62.22
	PSNR	29.29	29.1	30.19
POCS	MSE	64.54	142.29	56.8
	PSNR	30.03	26.6	30.59

Table B.6 shows the MSE and PSNR of Test image 2 for different motion estimation algorithm recovered with different SR reconstruction algorithms.

Test image 3

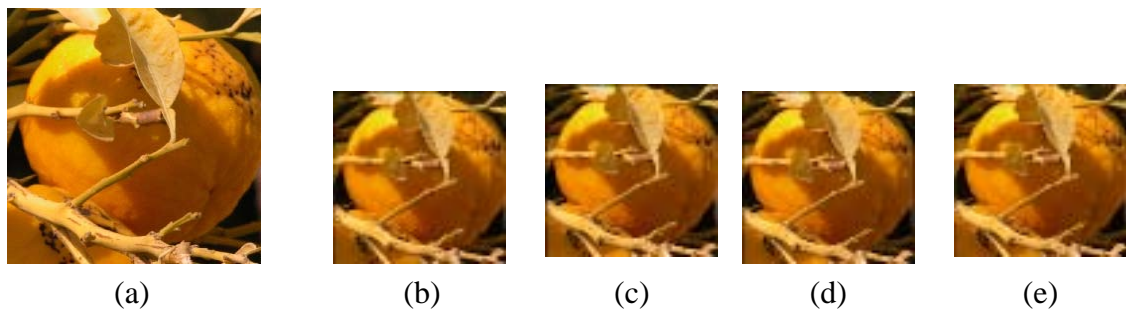


Figure B.3: Original and transformed images (a) HR image (b) down sampled, no transformation (c)  $0.1^0$ , (0.1747, 0.8351) pix (d)  $0.1^0$ , (0.2709, 0.4276) pix (e)  $0.1^0$ , (0.6567, 0.0739) pix LR images

Table B.7: List of different HR images using different registration and reconstruction algorithms

Algorithms	Vandewalle	Marcel	Keren
Interpolation			
Papoulis Gerchberg			
Iterated Back Projection (IBP)			
Robust Super Resolution			
Projection onto Convex Sets (POCS)			

Above figure B.3 shows original HR image and differently transformed LR images. These transformation parameters are entered manually and corresponding LR images are

generated using MATLAB. Using different registration algorithm, different SR algorithms are implemented to test image 3 and above table shows all the results.

Table B.8: Manually entered transformation parameters

Rotation	Translation	
Angle (in degree)	x	y
0	0	0
0.1	0.1747	0.8351
0.1	0.2709	0.4276
0.1	0.6567	0.0739

For four LR images to generate four different parameters are entered manually. First image is not transformed so inputs are  $0^0$  and (0, 0) pixel shifts and other three are transformed using above table data.

Table B.9: MSE and PSNR of Test image 3 for different algorithms

Algorithms	Error	Vandewalle	Marcel	Keren
Interpolation	MSE	31.83	60.73	32.07
	PSNR	33.1	30.3	33.07
Papoulis Gerchberg	MSE	126.94	181.84	105.17
	PSNR	27.09	25.53	27.91
Iterated Back Projection	MSE	47.17	54.79	51.45
	PSNR	31.39	30.74	31.02
Robust Super Resolution	MSE	42.36	49.73	73.94
	PSNR	31.86	31.16	29.44
POCS	MSE	43.17	101.93	41.57
	PSNR	31.78	28.05	31.94

Table B.9 shows the MSE and PSNR of Test image 3 for different motion estimation algorithm recovered with different SR reconstruction algorithms.



Test image 4



Figure B.4: Original and transformed images (a) HR image (b) down sampled, no transformation (c)  $0.1^0$ , (0.1747, 0.8351) pix (d)  $0.1^0$ , (0.2709, 0.4276) pix (e)  $0.1^0$ , (0.6567, 0.0739) pix LR images

Table B.10: List of different HR images using different registration and reconstruction algorithms

Algorithms	Vandewalle	Marcel	Keren
Interpolation			
Papoulis Gerchberg			
Iterated Back Projection (IBP)			
Robust Super Resolution			
Projection onto Convex Sets (POCS)			

Above figure B.4 shows original HR image and differently transformed LR images. These transformation parameters are entered manually and corresponding LR images are generated using MATLAB. Using different registration algorithm, different SR algorithms are implemented to test image 4 and above table shows all the results.

Table B.11: Manually entered transformation parameters

Rotation	Translation	
Angle (in degree)	x	y
0	0	0
0.1	0.1747	0.8351
0.1	0.2709	0.4276
0.1	0.6567	0.0739

For four LR images to generate four different parameters are entered manually. First image is not transformed so inputs are  $0^0$  and (0, 0) pixel shifts and other three are transformed using above table data.

Table B.12: MSE and PSNR of Test image 4 for different algorithms

Algorithms	Error	Vandewalle	Marcel	Keren
Interpolation	MSE	42.18	64.42	41.6
	PSNR	31.88	30.04	31.94
Papoulis Gerchberg	MSE	120.3	177.12	105.73
	PSNR	27.33	25.65	27.89
Iterated Back Projection	MSE	54.94	61.51	95.25
	PSNR	30.73	30.24	28.34
Robust Super Resolution	MSE	85	57.57	74.93
	PSNR	28.84	30.53	29.38
POCS	MSE	49.29	96.24	49.14
	PSNR	31.2	28.3	31.22

Table B.12 shows the MSE and PSNR of Test image 4 for different motion estimation algorithm recovered with different SR reconstruction algorithms.

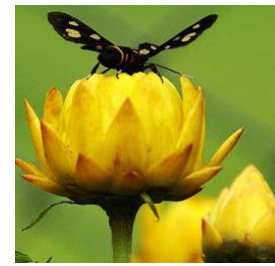
Test images



(a)















(b)



(c)

Figure B.5: Original HR Test images

Table B.13: HR image generation for noisy images

Noise (in db)	POCS		
10			
20			
30			
40			

Above table B.13 shows the image reconstruction of three different noisy images recovered through POCS algorithm with Keren registration.

Table B.14: MSE and PSNR of Test images

Noise (in db)	Error	POCS Algorithm		
10	MSE	54.07	82.6	55.04
	PSNR	30.84	28.99	30.76
20	MSE	40.1	86.79	47.14
	PSNR	32.13	28.79	31.43
30	MSE	44.39	81.26	45.67
	PSNR	31.69	29.07	31.57
40	MSE	41.09	84.53	43.78
	PSNR	32.03	28.89	31.75

Table B.14 shows the MSE and PSNR of test images with different noise levels shown in figure B.5 using Keren motion estimation algorithm recovered with POCS reconstruction algorithm.

## Appendix C

### Datasets

Datasets are taken from the web site [WWW.vasc.ri.cmu.edu/idb/html/motion/index.html](http://WWW.vasc.ri.cmu.edu/idb/html/motion/index.html)

Test image 1

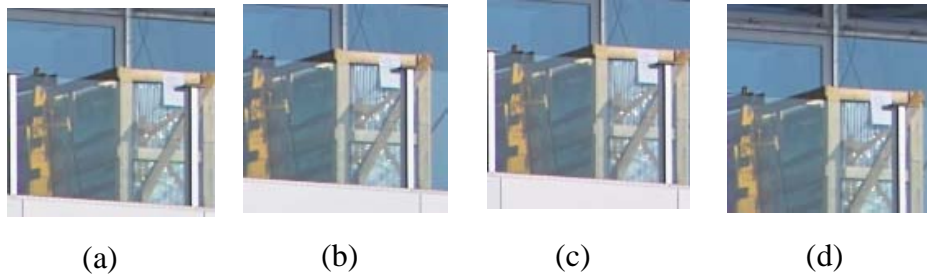


Figure C.1: Real LR Test images

Table C.1: List of different HR images using different registration and reconstruction algorithms

Algorithms	Vandewalle	Marcel	Keren
<b>Interpolation</b>			
<b>Papoulis Gerchberg</b>			
<b>Iterated Back Projection (IBP)</b>			
<b>Robust Super Resolution</b>			
<b>Projection onto Convex Sets (POCS)</b>			

Test mage 2

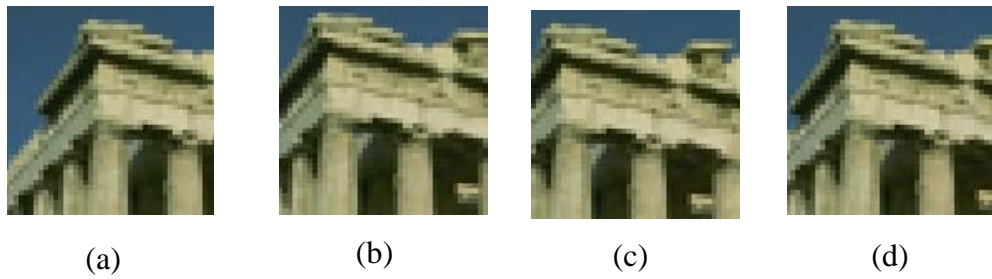


Figure C.2: Real LR Test images

Table C.2: List of different HR images using different registration and reconstruction algorithms

<b>Algorithms</b>	<b>Vandewalle</b>	<b>Marcel</b>	<b>Keren</b>
<b>Interpolation</b>			
<b>Papoulis Gerchberg</b>			
<b>Iterated Back Projection (IBP)</b>			
<b>Robust Super Resolution</b>			
<b>Projection onto Convex Sets (POCS)</b>			

Test image 3

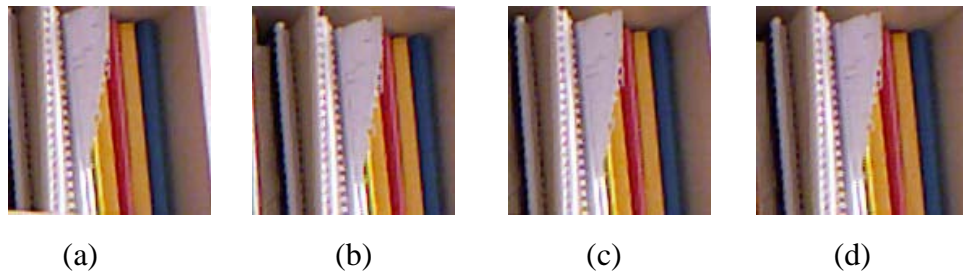


Figure C.3: Real LR Test images

Table C.3: List of different HR images using different registration and reconstruction algorithms

<b>Algorithms</b>	<b>Vandewalle</b>	<b>Marcel</b>	<b>Keren</b>
<b>Interpolation</b>			
<b>Papoulis Gerchberg</b>			
<b>Iterated Back Projection (IBP)</b>			
<b>Robust Super Resolution</b>			
<b>Projection onto Convex Sets (POCS)</b>			

Above figures show real LR image with unknown transformation, unknown blur and noise. Using different registration algorithm, different SR algorithms and finally applying median filter are implemented to test images 1, 2 and 3. These images are demonstrated on tabular format.